Method of Sentinels for Packing Objects within Arbitrary Regions

E. G. Birgin * J. M. Martínez † W. F. Mascarenhas ‡ D. P. Ronconi §

May 23, 2005

Abstract

A new method is introduced for packing objects in convex regions of the Euclidian n-dimensional space. By means of this approach the packing problem becomes a global finite-dimensional continuous optimization problem. The strategy is based on the new concept of sentinels sets. Sentinels sets are finite subsets of the objects to be packed such that when two objects are superposed at least one sentinel of one object is in the interior of the other. Minimal sets of sentinels are found in simple $2-$dimensional cases. Numerical experiments and pictures showing the potentiality of the new technique are presented.

Keywords: Sentinels, packing problems, cutting problems, models, nonlinear programming.

1 Introduction

The problem of packing a given set of pieces into defined regions maximizing the total number of pieces or the used area occurs in a large range of practical situations, including manufacturer's pallet loading, packing of ship containers and establishing of layout in clothing industry. Many papers have been published dealing with packing problems. A useful classification has been given by Dyckhoff [14]. One of the most popular and useful problem in this area is to find the maximum number of rectangles that can be orthogonally packed into a larger rectangle. Polynomial algorithms for the guillotine version of the problem exist [32] whereas the NP-completeness of the non-guillotine problem has been conjectured [15, 28]. In [24] a very efficient heuristic to solve this problem was introduced. The authors conjectured that their method

*Department of Computer Science IME-USP, University of São Paulo, Rua do Matão 1010, Cidade Universitária, 05508-090, São Paulo SP, Brazil. This author was supported by PRONEX-Optimization 76.79.1008-00, FAPESP (Grants 01-04597-4 and 02-00094-0) and CNPq (Grant 300151/00-4). Corresponding author. FAX: +55(11)3091-6134. e-mail: egbirgin@ime.usp.br

†Department of Applied Mathematics, IMECC-UNICAMP, University of Campinas, CP 6065, 13081-970 Campinas SP, Brazil. This author was supported by PRONEX-Optimization 76.79.1008-00, FAPESP (Grant 01-04597-4), CNPq and FAEP-UNICAMP. e-mail: martinez@ime.unicamp.br

‡Department of Computing and Statistics, UFMS, Federal University of Mato Grosso do Sul, CP 549, 79070-900 Campo Grande MS, Brazil. e-mail: walter@geocad.com.br

§Department of Production Engineering, EP-USP, University of São Paulo, Av. Prof. Almeida Prado, 128, Cidade Universitária, 05508-090, São Paulo SP, Brazil. This author was supported by FAPESP (Grants 00-01715-3 and 01-02972-2). e-mail: dronconi@usp.br

always finds an optimal solution and solved hard instances that remained unsolved by other heuristics.

Several mixed 0-1 integer linear and nonlinear programming models have been proposed for 2D and 3D packing problems in which identical or non-identical boxes must be packed into a bigger box. In general, the packed boxes can be rotated, but always with its sides parallel to the sides of the bigger box. Sometimes constraints are imposed related to the number of each type of box being packed. In general, the proposed models are difficult. When an exact method is used, large-scale problems become impossible to solve. Fortunately, heuristic methods find optimal or good quality solutions in many cases. See, for example, [3, 4, 12, 13, 20, 33].

In [4] a nonlinear formulation for the constrained two-dimensional non-guillotine cutting problem is presented and the model is used for the elaboration of a populational heuristic. The proposed model has two main difficulties: (i) the presence of integer variables; and (ii) the non-differentiability of the nonlinear constraints used to avoid overlapping. The first difficulty may be circumvented by replacing constraints of type $x \in \{0, 1\}$ by $x(1 - x) = 0$. However, this kind of constraints leads to hard-to-solve nonlinear problems with many local-nonglobal solutions. Several strategies for fixing integer variables and solving the problem as a sequence of continuous nonlinear problems have also been proposed. The second inconvenient of the formulation can be overcome by approximating the nonsmooth constraints by smooth ones. These two ideas lead to nonlinear formulations that are suitable for classical nonlinear optimization solvers.

Several works related to packing irregular polygons have been also published. Most of them are based on placement policies previously defined (for example, bottom-left) and aim to find optimal solutions related to the pre-established policy. In [5] an easy way to compute a placement policy known as "non-fit polygon" has been proposed. This idea is used in [17], among other strategies, to develop a bottom-left placement algorithm for polygon packing. See also [1, 16, 22, 23].

The Method of Sentinels introduced in this paper is a procedure for packing objects inside a convex region without overlapping. The main idea is to define a set of points called sentinels for each small object in such a way that two objects are superposed if and only if at least a sentinel of one of the objects is in the interior of the other object. Based on the sentinels sets, a smooth nonlinear decision model to determine if a fixed set of objects can be packed inside the convex region without overlapping is defined. The variables of the model are the ones that define a displacement in the Euclidian space. In 2D problems, the displacement is defined by a vector of translation and an angle of rotation. So, the method is not restricted to orthogonal (parallel to the axes) patterns. The new concept of sentinels introduces some difficult theoretical problems related to identification and minimality. Here we present minimal sets of sentinels for the case of identical rectangles and regular polygons. More general objects, convex or non-convex, obtained by combination of identical rectangles are also considered. The non-linear decision model is solved using the well-established bound-constrained solver GENCAN [6].

This paper is organized as follows. In Section 2 the Method of Sentinels for packing objects on arbitrary regions is introduced. In Section 3 we define an optimal set of sentinels for rectangular objects and regular polygons. In Section 4 we present numerical experiments using the Method of Sentinels for packing rectangular objects on arbitrary convex regions. In Section 5 we state conclusions and lines for future research. In the Appendix we collect the technical proofs and theorems stated in Section 3.

2 Using Sentinels for Packing

We begin with an informal and general description of the Method of Sentinels. Let A_1 and A_2 be nonempty, open, bounded and convex sets of $\mathbb{R}^n$. Sets with these characteristics will be called *objects* from now onwards. Define $B_1 = \bar{A}_1$ the closure of A_1 and $B_2 = \bar{A}_2$ the closure of A_2. Let $D_1, D_2 : \mathbb{R}^n \to \mathbb{R}^n$ be two displacement operators. So, D_1 and D_2 transform objects in objects preserving distances, angles and orientation. If $D_1(A_1) \cap D_2(A_2) \neq \emptyset$ then we say that $D_1(B_1)$ and $D_2(B_2)$ (or $D_1(A_1)$ and $D_2(A_2)$) are *superposed*.

Let S_1 and S_2 be finite subsets of B_1 and B_2 respectively. We say that S_1 and S_2 are *sentinels sets* relatively to B_1 and B_2 if the following property holds:

For all displacements D_1, D_2, if $D_1(B_1)$ and $D_2(B_2)$ are superposed, then

$$D_1(S_1) \cap D_2(A_2) \neq \emptyset \text{ or } D_2(S_2) \cap D_1(A_1) \neq \emptyset. \tag{1}$$

Roughly speaking, if, after the displacements, the objects B_1 and B_2 are superposed, then at least one sentinel of B_1 becomes interior to B_2 or one sentinel of B_2 becomes interior to B_1.

Now, assume that $B_1, \ldots, B_m \subset \mathbb{R}^n$, $\Omega \subset \mathbb{R}^n$ and we want to *pack* the objects $B_1, \ldots, B_m$ into the region Ω. This means that we want to find displacements $D_1, \ldots, D_m$ such that

$$D_j(B_j) \subset \Omega \; \forall \, j = 1, \ldots, m \tag{2}$$

and

$$D_i(B_i) \text{ and } D_j(B_j) \text{ are not superposed } \; \forall \, i, j = 1, \ldots, m, \; i \neq j. \tag{3}$$

Assume that $S_1 \subset B_1, \ldots, S_m \subset B_m$ are such that S_i and S_j are *sentinels sets* relatively to B_i and B_j. For all $i, j = 1, \ldots, m, \; i \neq j$, define

$$\kappa(D_i, D_j) = \#\{[D_i(S_i) \cap D_j(A_j)] \cup [D_j(S_j) \cap D_i(A_i)]\}. \tag{4}$$

Then, condition (3) can be formulated as follows:

$$\kappa(D_i, D_j) = 0 \; \forall \, i, j = 1, \ldots, m, \; i \neq j. \tag{5}$$

So, the packing problem defined by (2)-(3) is related to the optimization problem

$$\text{Minimize } \sum_{i \neq j} \kappa(D_i, D_j) \;\; \text{s. t.} \;\; D_k(B_k) \subset \Omega \; \forall \, k = 1, \ldots, m. \tag{6}$$

If a global solution of (6) is found such that the objective function value vanishes, then the packing problem (2)-(3) is solved. The objective function of (6) represents the total number of sentinels of one object that, after the displacements, fall in the interior of some other object.

The optimization problem (6) defines the Method of Sentinels. However, this minimization problem needs to be reformulated in order to transform it into a solvable nonlinear programming problem. Let us consider the case in which Ω is a closed and convex set defined by a set of inequalities. So,

$$\Omega = \{x \in \mathbb{R}^n \mid g_i(x) \leq 0, \; i = 1, \ldots, p\}. \tag{7}$$

Moreover, assume that each object B_k is a bounded polytope, so it is the convex hull of its vertices $V_1(B_k), \dots, V_{\nu(k)}(B_k)$. Then, the constraints of (6) take the form

$$g_i(D_k[V_\ell(B_k)]) \leq 0 \; \forall \; \ell = 1, \dots, \nu(k), k = 1, \dots, m, i = 1, \dots, p. \tag{8}$$

The displacements D_k can always be described by a finite set of parameters. For example, displacements in $\mathbb{R}^2$ are given by three parameters, the first two representing a translation and the third the angle of rotation. Displacements in $\mathbb{R}^3$ are given by three translation parameters and two angles of rotation, and so on. Therefore, the constraints (8) have the usual form adopted in nonlinear programming problems.

Let us analyze now the objective function of (6). This function depends on the continuous variables that define the displacements but it takes only discrete integer nonnegative values. For nonlinear programming reformulations we need to replace it by a continuous function of the displacement variables. As before, we restrict ourselves to the case in which the sets B_k are bounded polytopes. In this case, B_k is described by a set of linear inequalities:

$$\langle c_{k,j}, x \rangle \leq b_{k,j}, \; j = 1, \dots, \mu(k). \tag{9}$$

If s is a sentinel of B_i and $D_i(s)$ is in $D_k(A_k)$ with $k \neq i$, then $D_k^{-1} D_i(s)$ belongs to A_k and, so, it satisfies:

$$\langle c_{k,j}, D_k^{-1} D_i(s) \rangle < b_{k,j}, \; j = 1, \dots, \mu(k). \tag{10}$$

Thus, the displaced sentinel s belongs to the displaced A_k if, and only if,

$$\prod_{j=1}^{\mu(k)} \max\{0, b_{k,j} - \langle c_{k,j}, D_k^{-1} D_i(s) \rangle\} > 0. \tag{11}$$

Therefore, a degree of the superposition of B_i and B_k under the displacements D_i and D_k is given by

$$\Phi(D_i, D_k) = \tag{12}$$

$$\sum_{s \in S_i} \prod_{j=1}^{\mu(k)} [\max\{0, b_{k,j} - \langle c_{k,j}, D_k^{-1} D_i(s) \rangle\}]^2 + \sum_{s \in S_k} \prod_{j=1}^{\mu(i)} [\max\{0, b_{i,j} - \langle c_{i,j}, D_i^{-1} D_k(s) \rangle\}]^2$$

The function $\Phi(D_i, D_k)$ is nonnegative and continuously differentiable with respect to the parameters that define the displacements D_i and D_k and it vanishes if, and only if, $D_i(B_i)$ and $D_k(B_k)$ are not superposed. Therefore, it can replace the function κ in the optimization problem (6).

Summing up, in the case in which Ω is a convex set defined by inequalities and the objects are bounded polytopes, the packing problem can be formulated as the following nonlinear programming problem:

$$\text{Minimize } \sum_{i \neq j} \Phi(D_i, D_j) \tag{13}$$

subject to (8). Moreover, since we are only interested in global solutions of (13) where the objective function must vanish, the problem can be reformulated as the feasibility problem given below:

$$\sum_{i \neq j} \Phi(D_i, D_j) = 0, \tag{14}$$

$$g_i(D_k[V_\ell(B_k)]) \leq 0 \; \forall \; \ell = 1, \ldots, \nu(k), k = 1, \ldots, m, i = 1, \ldots, p. \tag{15}$$

Finally, (14)-(15) is equivalent to the following unconstrained continuously differentiable global optimization problem:

$$\text{Minimize } \sum_{i \neq j} \Phi(D_i, D_j) + \sum_{i=1}^{p} \sum_{k=1}^{m} \sum_{\ell=1}^{\nu(k)} [\max\{0, g_i(D_k[V_\ell(B_k)])\}]^2. \tag{16}$$

3 Sentinels for Planar Polygons

Let us restrict ourselves to 2D packing problems of polygons. We present examples of polygons for which any set of sentinels is infinite and characterize a class of polygons that have finite sets of sentinels. We explain how to build sentinel sets for polygons in this last class and also provide optimal sentinel sets for rectangles and regular polygons. The proofs of all lemmas and theorems presented in this section can be found in the Appendix.

In this section we work with *polygons*, by which we mean a sequence of points $p_0, p_1, \ldots, p_{n-1}$ connected by segments $p_i p_{i+1}$ that do not cross. The only contact the segments have is at the vertices p_i. We also assume that no three consecutive points p_i are aligned and use the indices modulo the number of points in P. According to this definition, polygons are not open sets. However, in order to simplify the language, we will say that $S_1, \ldots, S_n$ is a set of sentinels for a family of polygons $P_1, \ldots, P_n$ even when, to be one hundred percent rigorous, we should say that $S_1, \ldots, S_n$ is a set of sentinels for *the interior* of $P_1, \ldots, P_n$.

We are now ready to state a negative result: triangles do not have finite sentinel sets. In fact, any two polygons with an internal angle smaller than $\pi/2$ that could be superposed like in Figure 1, with contact only at the acute tips, cause problems. In this case, one can place any finite number of sentinels near the touching tips and it will always be possible to move the polygons slightly and have them to intersect in such way that one polygon does not touch the sentinels of the other.

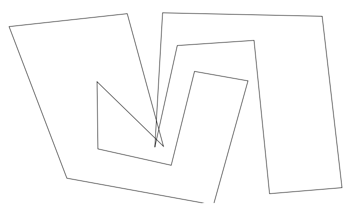

Figure 1: Polygons with internal angles smaller than $\pi/2$ may not have finite sets of sentinels.

On the other hand, this is as bad as things may get, as stated in the next theorem:

Theorem 1 *If $P_1, \ldots, P_n$ is a family of n planar polygons such that all internal angles of all P_i's are bigger than or equal to $\pi/2$ then there exist a family of finite sets of sentinels $S_1, \ldots, S_n$ for $P_1, \ldots, P_n$.*

The sentinel sets used to prove this theorem are built in two steps. First we use the next two lemmas to reduce the problem to the convex case:

Lemma 1 *Every polygon with internal angles bigger than or equal to $\pi/2$ can be decomposed as the union of convex polygons with internal angles bigger than or equal to $\pi/2$.*

Lemma 2 *Let $A_1, \ldots, A_n$ be a family of open sets such that each A_i is decomposed as $A_i = \cup_{j=1}^{n_i} A_{ij}$, for some open sets A_{ij}. Consider the set of n-uples $K = \{(k_1, \ldots, k_n)$ with $1 \leq k_i \leq n_i$ for $i = 1, \ldots, n\}$. If $S_{1k_1}, S_{2k_2}, \ldots, S_{nk_n}$ are sentinels sets for $A_{1k_1}, A_{2k_2}, \ldots A_{nk_n}$ for all $(k_1, \ldots, k_n) \in K$ then the sets $S_i = \cup_{j=1}^{n_i} S_{ij}$ are sentinels sets for $A_1, \ldots, A_n$.*

In words, Lemma 2 states that we can obtain sentinels sets for the whole set by combining the sentinels sets for their parts. As a consequence of the last two lemmas, we mostly care about convex polygons and the next lemma is of interest:

Lemma 3 *If $P_1, \ldots, P_n$, $n \geq 2$, is a family of strictly convex polygons and $S_1, \ldots, S_n$ is a family of finite sets of sentinels for the P_i's then each S_i contains all the vertices of P_i.*

Thus, vertices are natural candidates to sentinels. Moreover, in the case when some P_i are repeated we must have internal sentinels. Otherwise we could just put one copy right above the other. This observation proves the following lemma.

Lemma 4 *Let $A_1, \ldots, A_n$ be a family of open sets and $S_1, \ldots, S_n$ be a family of finite sets of sentinels for the A_i's. If $A_i = A_j$ for $i \neq j$ then $(S_i \cap A_i) \cup (S_j \cap A_j) \neq \emptyset$.*

We are now ready to explain the construction used to prove Theorem 1. First we decompose each polygon as the union of convex parts with internal angles bigger than or equal to $\pi/2$. We take the vertices of such parts as sentinels. Next, for each convex part $C = c_0 c_1 \ldots c_k$, $c_k = c_0$, we take an arbitrary internal sentinel in the set

$$I = \bigcap_{i=1}^{k} C_i,$$

where C_i is the convex polygon with vertices c_j with $j \neq i$. Each C_i is the convex set obtained from C by the removal of the ear $c_{i-1} c_i c_{i+1}$ and their intersection is illustrated in Figure 2.

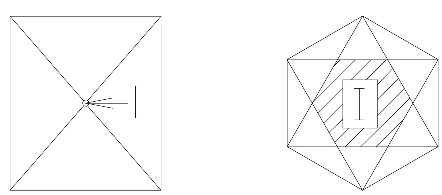

Figure 2: The set I for the rectangle (just one point) and the hexagon (hatched).

Since each C has at least four vertices, Helly's theorem implies that I is not empty, because the intersection of any three C_i's, for $i \in \{i_1, i_2, i_3\}$, contains at least a vertex c_j for some $j \notin \{i_1, i_2, i_3\}$. Therefore, we can always pick an internal sentinel for C as described above.

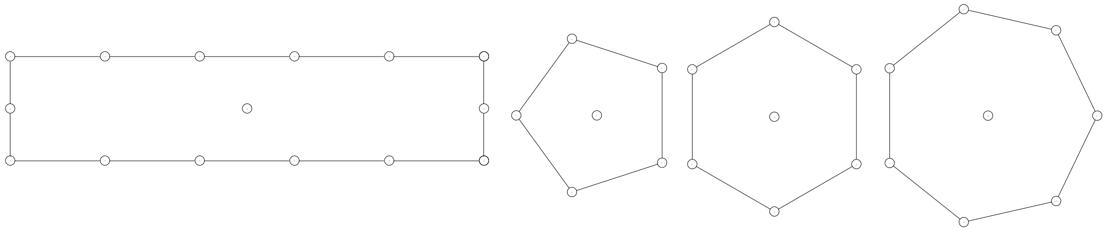

Figure 3: A family of polygons and their sentinels. The rectangle has smallest side of length slightly bigger than 1 and the other polygons have sides of length 1. The sentinels in the borders are 1 apart, except for the ones in the smallest side of the rectangle, which are roughly 1/2 apart.

Finally we take a small δ and populate the sides of the parts with sentinels which are at most δ apart, as in Figure 3. In the case when no polygon has parallel sides which are close to each other we can take δ as the length of the smallest side among all the polygons. In cases similar to the rectangle, when there are two consecutive internal angles of $\pi/2$, we must take δ slightly smaller than the side connecting the corresponding vertices. To be precise, we can take any δ smaller than the length of any segment xy connecting nonconsecutive sides of one of the polygons P_i and such that the relative interior of xy is contained in the interior of P_i, as formalized in the definition of *splitting segment*, which is illustrated in Figure 4

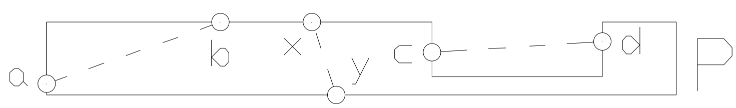

Figure 4: The segment xy splits P but ab does not, because its endpoints are in consecutive sides. The segment cd does not split P because a part of it lies outside the interior of P.

Definition 1 *We say that a segment xy with endpoints in nonconsecutive sides of a polygon P splits P if the relative interior of xy is contained in the interior of P, i.e, if xy is contained in P and splits it in two polygons which are not triangles.*

The construction in the last paragraphs shows that Theorem 1 is a corollary of the following general theorem.

Theorem 2 *If P_1, ..., P_n is a family of polygons with internal angles bigger than or equal to $\pi/2$ and $S_i = B_i \cup I_i$, for $i = 1, \ldots, n$, is a collection of sets and δ is a number such that*

1. *Any segment that splits any P_i has length bigger than δ.*
2. *The points of B_i are in the border of P_i and the vertices of P_i belong to B_i.*
3. *For any p in the border of P_i there exist $x, y \in B_i$ such that $\|x - y\| \leq \delta$ and p is in the segment xy.*

4. I_i is contained in interior of P_i and any p in the interior of P_i is visible from some $x \in I_i$, that is, for any p in the interior of P_i there exists $x \in I_i$ such that the segment xp is contained in the interior of P_i.

5. If the polygon P_i has vertices $p_{i0}, p_{i1}, \ldots, p_{ik} = p_{i0}$ then the intersection of I_i with the interior of the triangles $p_{ij}p_{i(j+1)}p_{i(j+2)}$ is empty (indexes taken modulo k.)

then $S_1, \ldots, S_n$ is a family of sentinels sets for the P_i's.

The reader can verify that the points indicated in Figure 3 satisfy all the conditions for Theorem 2, corroborating our claim that they are sentinels sets for these sets. Notice also that there is no condition regarding convexity in Theorem 2. In fact, our construction uses the reduction to convex sets only to guarantee the existence of the internal sentinels that "see" all the polygon and lie outside of its ears $p_j p_{j+1} p_{j+2}$.

Lemmas 3 and 4 show that the sets of sentinels we propose are optimal for families of regular polygons with sides of the same length and with more than four vertices. However, the case for rectangles is different. Since rectangles are so important in practice we devote the last part of this section to them. We will present optimal sets of sentinels for families $R_1, \ldots, R_n$ of identical rectangles. Our analysis is based on what we call "dual approach" and may also be used to analyze more general situations. In the next paragraphs we give an heuristic overview of this approach. At the end of the section we explain how to use the dual approach to build optimal sentinel sets for the rectangles and provide rigorous proofs in this case.

The dual approach relates sentinels to a covering problem, which is, in some sense, dual to the main subject of this work: packing problems. To establish this connection, notice that any displacement of a set $C \in I\!\!R^2$ can be written in matrix-vector form as

$$C_{\theta d} = d - H_\theta C, \tag{17}$$

where d is a vector in $I\!\!R^2$ and H_θ is the counterclockwise rotation by the angle θ:

$$H_\theta = \begin{pmatrix} \cos\theta & -\sin\theta \\ \sin\theta & \cos\theta \end{pmatrix}. \tag{18}$$

Let us suppose that we are deciding if $\widehat{U}$ and $\widehat{V}$ are sentinel sets for a pair of open sets $U, V \in I\!\!R^2$ (notice that our candidates to sentinel wear hats). In this case we would need to convince ourselves that

$$U \cap V_{\theta d} \neq \emptyset \Rightarrow (U \cap \widehat{V}_{\theta d}) \cup (\widehat{U} \cap V_{\theta d}) \neq \emptyset, \tag{19}$$

that is, if U intercepts the displaced V then either U intercepts the displaced $\widehat{V}$ or $\widehat{U}$ intercepts the displaced V. The condition $U \cap V_{\theta d} \neq \emptyset$ is equivalent to the existence of $u \in U$ and $v \in V$ such that

$$u = d - H_\theta v.$$

On the other hand, $U \cap \widehat{V}_{\theta d} \neq \emptyset$ is equivalent to the existence of $u' \in U$ and $\widehat{v} \in \widehat{V}$ such that

$$u' = d - H_\theta \widehat{v},$$

and $\widehat{U} \cap V_{\theta d}$ corresponds to the existence of $v' \in V$ and $\widehat{u} \in \widehat{U}$ such that

$$\widehat{u} = d - H_\theta v'.$$

Thus, if we put θ in a second plane and focus on d, the expression (19) is equivalent to

$$\mathcal{D}_\theta(U, V) \subset \mathcal{D}_\theta(U, \widehat{V}) \cup \mathcal{D}_\theta(\widehat{U}, V), \tag{20}$$

for $\mathcal{D}_\theta(.,.)$ defined similarly in the three cases:

$$\mathcal{D}_\theta(U, V) \;=\; \{d \in I\!R^2 \mid d = u + H_\theta v, \text{ for } u \in U \text{ and } v \in V\}, \tag{21}$$
$$\mathcal{D}_\theta(U, \widehat{V}) \;=\; \{d \in I\!R^2 \mid d = u' + H_\theta \widehat{v}, \text{ for } u' \in U \text{ and } \widehat{v} \in \widehat{V}\}, \tag{22}$$
$$\mathcal{D}_\theta(\widehat{U}, V) \;=\; \{d \in I\!R^2 \mid d = \widehat{u} + H_\theta v', \text{ for } \widehat{u} \in \widehat{U} \text{ and } v' \in V\}. \tag{23}$$

Under the assumptions made upon U,V and the candidate sentinel sets $\widehat{U}$ and $\widehat{V}$, the reverse of (20), that is $\mathcal{D}_\theta(U, V) \supset \mathcal{D}_\theta(U, \widehat{V}) \cup \mathcal{D}_\theta(\widehat{U}, V)$ always holds. Therefore, the distinction of sentinel sets and arbitrary sets can be made by checking if

$$\mathcal{D}_\theta(U, V) = \mathcal{D}_\theta(U, \widehat{V}) \cup \mathcal{D}_\theta(\widehat{U}, V) \tag{24}$$

for all θ. This situation is depicted in Figure 5

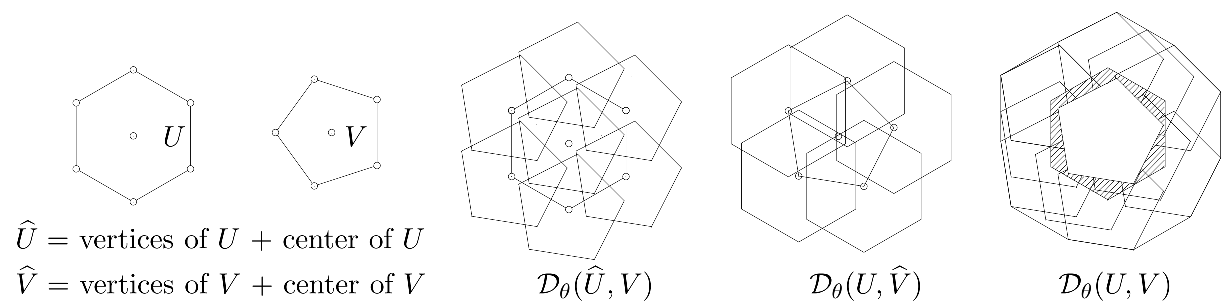

Figure 5: Example of sets $U, V, \widehat{U}, \widehat{V}$ and their duals $\mathcal{D}_\theta(\widehat{U}, V)$,$\mathcal{D}_\theta(U, \widehat{V})$ and $\mathcal{D}_\theta(U, V)$.

The dual set $\mathcal{D}_\theta(\widehat{U}, V)$ is obtained attaching a displaced copy of V to each element of $\widehat{U}$, $\mathcal{D}_\theta(U, \widehat{V})$ is obtained attaching copies of U to the displaced elements of $\widehat{V}$ and $\mathcal{D}_\theta(U, V)$ is obtained attaching a displaced copy of V to each element of U. Notice that by definition $\mathcal{D}_\theta(U, V)$ is the union of an infinite family of sets but, since $\widehat{U}$ and $\widehat{V}$ are sentinels for U and V, it is also the union of the finite families that form $\mathcal{D}_\theta(U, \widehat{V})$ and $\mathcal{D}_\theta(U, \widehat{V})$. Therefore, $\widehat{U}$ and $\widehat{V}$ are sentinels for U and V if and only if, for each θ, the finite families that define $\mathcal{D}_\theta(U, \widehat{V})$ and $\mathcal{D}_\theta(\widehat{U}, V)$ cover the whole dual $\mathcal{D}_\theta(U, V)$.

The dual formulation leads to a simple heuristics to check if $\widehat{U}$ and $\widehat{V}$ are sentinels for U and V: discretize the interval $[0, 2\pi)$ in small intervals with width $\delta\theta$ and check the condition (20) for every $\theta = k\delta\theta$. This can be done visually, using a CAD program, or automatically, by software. In fact, it could even be turned into a rigorous automated procedure, to prove things, if exact arithmetic were used and some properties of the dual sets were explored. However, a more detailed discussion of this topic would take us to far from our main route.

Using the sentinel approach, with visual inspection for several values of θ in the software AutoCAD, we found the following optimal sentinel sets when all the P_i's equal the rectangle R_λ with vertices $(\pm\lambda, \pm 1)$ and $\lambda \geq 1$.

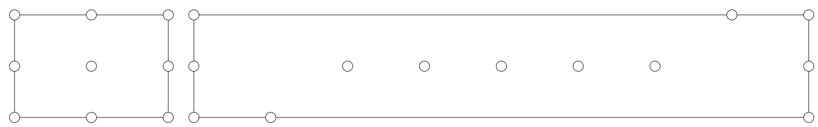

Figure 6: The minimal sentinel set S_λ for the rectangle R_λ.

For technical reasons, we must look at two ranges for λ: $\lambda < 4$ and $\lambda \geq 4$, and the horizontal distance δ^λ among the points is at most

$$\delta^\lambda = \lambda/2 \quad \text{if } 1 \leq \lambda < 4, \tag{25}$$

$$\delta^\lambda = \frac{2\lambda}{\lfloor \lambda \rfloor + 1} \text{ if } \lambda \geq 4. \tag{26}$$

Formally we define two sentinel sets, the one above, S_λ, and its reflection T_λ on the x axis. These sets are defined in terms of the auxiliary sets M^λ and B^λ as follows

$$B^\lambda = \{(-\lambda, -1), (-\lambda, 0), (-\lambda, 1), (\lambda, -1), (\lambda, 0), (\lambda, 1)\}, \tag{27}$$

$$M^\lambda = \{(k\delta^\lambda - \lambda, 0), \text{ for } 2 \leq k \leq n^\lambda + 1\}, \tag{28}$$

$$n^\lambda = 1 \text{ for } \lambda < 4 \text{ and } n^\lambda = \lfloor \lambda \rfloor - 2 \text{ otherwise}, \tag{29}$$

$$S_\lambda = B^\lambda \cup M^\lambda \cup \{(-\lambda + \delta^\lambda, -1), (\lambda - \delta^\lambda, 1)\}, \tag{30}$$

$$T_\lambda = B^\lambda \cup M^\lambda \cup \{(-\lambda + \delta^\lambda, 1), (\lambda - \delta^\lambda, -1)\}. \tag{31}$$

To round up our discussion of sentinels for the rectangle, we present the following technical results that at the end imply that our sentinels are indeed minimal. In the following lemmas and theorem we will be concerned with families in which all P_i's are equal to the rectangle R_λ and with sentinel sets that are equal too. In this case we say that S is a sentinel set for R_λ if $S, S, \ldots, S$ are sentinels for $R_\lambda, \ldots, R_\lambda$, for any given number of copies of R_λ and S. The first lemma specific for rectangles is this:

Lemma 5 *Every sentinel set of R_λ contains a point in the relative interior of each side of R_λ.*

Using the last lemma, Lemma 3 and Lemma 4 we deduce that every sentinel set of R_λ has at least 9 elements. However, for $\lambda \geq 4$ we have a sharper lower bound:

Lemma 6 *Every sentinel set of R_λ has at least $6 + \lfloor \lambda \rfloor$ elements.*

Theorem 3 *The sets S_λ and T_λ are sentinel sets for R_λ.*

According to (29), if $\lambda < 4$ then the number of elements of S_λ and T_λ is $8 + n^\lambda = 9$, which, as pointed out above, is the minimum number of sentinels for a rectangle. Otherwise, if $\lambda \geq 4$, then S_λ and T_λ have $8 + n^\lambda = 6 + \lfloor \lambda \rfloor$ elements, or the lower bound in Lemma 6. Therefore, our examples S_λ and T_λ of sentinel sets for the rectangle are optimal and our lower bounds on the number of elements in sentinel sets for rectangles are sharp.

4 Numerical Experiments

4.1 Basic Optimization Procedure

We solved problems of packing rectangles within arbitrary regions using the mathematical model (16). The unknowns of (16) are the translation vectors and the rotation angles for each rectangle. We imposed upper and lower bounds to the translation vectors. In general, these bounds are suggested by the problem which, frequently, imposes that the objects must be contained in a two-dimensional box. Therefore, (16) becomes a box-constrained smooth minimization problem. We use as sentinels the points of S_+^λ described in Section 3.

The box-constrained optimization problem was solved using GENCAN, an active set method that uses spectral projected gradients for leaving faces introduced in [6]. In general, the problem (16) has many local-nonglobal minimizers. In order to enhance the chance of convergence to global solutions we adopted the following strategies:

- **Improving initial approximation.** We took some circles that "almost cover" the rectangle as shown in Figure 7. Given an initial approximation for (16) we solved the problem of finding displacements such that the above mentioned circles do not intersect. For this, we used the same objective function used in [9] for the cylinder packing problem and in [26] for molecular packing and, once more, we employed GENCAN. This auxiliary problem is easier and less expensive than (16). Its minimizers (global or not) are not necessarily solutions of (16) but almost always provide improved initial points for solving our problem.

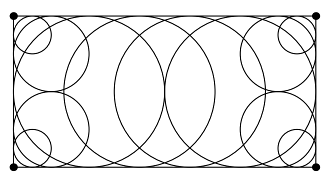

Figure 7: Partial covering of the rectangle by circles used to generate initial configurations.

- **Multistart procedure.** When the box-constrained solver does not find a set of displacements that pack the rectangles without overlapping, the objective function of (16) at the final approximation is strictly positive. In this case one does not know whether the packing problem is solvable or not. So, we try to solve (16) again using random starting displacements. The maximum number of trial initial configurations is specified in advance.

Let us mention the main implementation details:

- The center of the basic rectangle is the origin of $I\!R^2$. The initial translation vectors were chosen randomly in the feasible region. The initial rotation angles were chosen randomly between 0 and 2π.

- We tried to pack increasing number of rectangles in the desired region. The pictures exhibited indicate that we were not able to pack more rectangles than the exhibited ones.

- We tried a maximum of 1000 initial points for each problem.
- The parameters used in GENCAN were the default ones given in [6].

All the computations were done on an Intel Pentium III Computer with 256 Mb of RAM and 700MHz. Codes are in Fortran and the compiler used was GNU Fortran 2.95.2, with the optimization option "–O4".

4.2 Results

We solved the 30 problems described in Table 1. The solutions are given in Figures 8–14.

Problems 1–10 show how the method pack rectangles in arbitrary convex regions. In [25] the problem of packing containers in airplanes is analyzed. This practical problem is linked to the geometrical problems studied here.

Problems 11–18 consist in packing unitary squares in bigger squares. Problems 19–23 consist in packing unitary squares in equilateral triangles. Both problems are related to classical combinatorial and geometrical problems (see [18, 19]); namely, to find the smaller "big" square (or equilateral triangle) that contains a fixed number of "small" squares. The duality relationships between this problem and the one considered in this paper can be used to obtain approximations to the solution of the first.

Problems 24 and 25 show that our approach is able to obtain non-guillotine and guillotine solutions of the problem of packing rectangles in rectangles. It must be mentioned, however, that our method is not competitive with clever heuristics for orthogonal packing of rectangles in a big rectangle. See [24].

In Problems 26–29 we show how the method can be used to pack objects in regions that have prohibited zones [2, 10], when these zones can be described as unions of rectangles. In this case, the corresponding problem is handled using constraints that impose a fixed position to the rectangles that represent the forbidden regions.

Finally, observe that, at a first sight, in Problems 30, the packed objects are not rectangles [5, 17, 16, 1, 22, 23]. However, each object is also a union of rectangles and the desired configuration is obtained using the basic rectangle-packing procedure and imposing additional constraints to force that the packed rectangles preserve adequate relative positions. In other words, the problem of packing objects that are union of rectangles can be handled employing, essentially, the same technique introduced for rectangles.

5 Conclusions

In this paper we introduced the concept of *Sentinels Sets*. We proved the existence of finite sets of sentinels for polygons with their internal angles larger than or equal to $\pi/2$. Moreover, we found two minimal sets of sentinels to pack identical rectangles. An interesting and challenging problem is to find minimal sets of sentinels for arbitrary non-regular polygons or for 3D objects.

We introduced a nonlinear-programming oriented algorithm for packing objects in arbitrary regions. The method is based in the new concept of Sentinels Sets. To improve the efficiency of

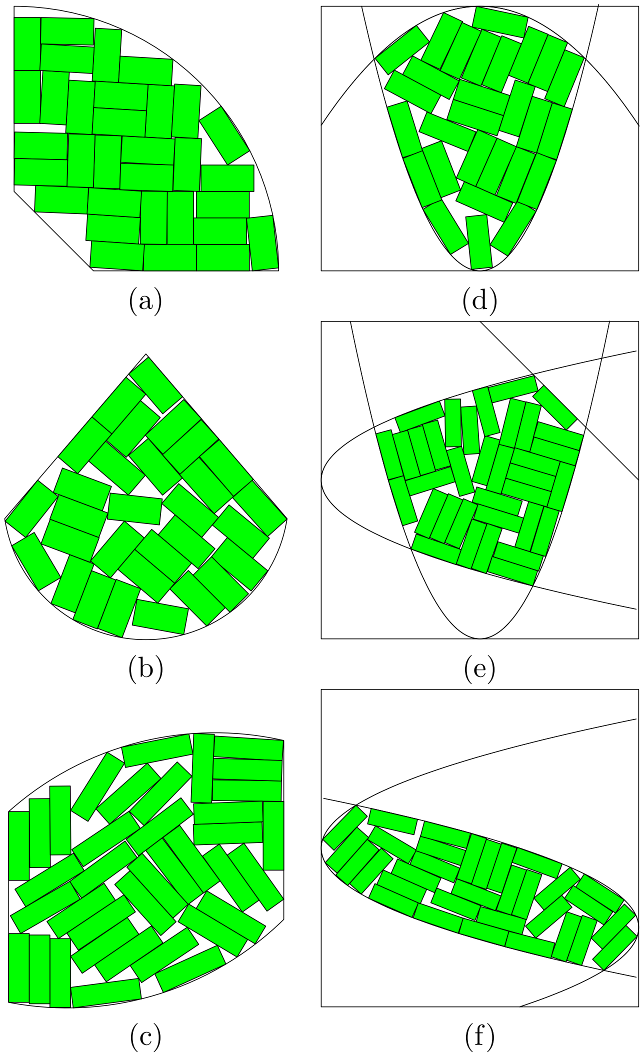

Figure 8: (a–c) Linear constraints and circles, (d–f) linear constraints and quadratics (Problems 1 to 6).

the proposed method the initial approximations are chosen using an auxiliary simpler nonlinear-programming procedure. However, the initial procedure alone is not able to find solutions of the packing problem and using the Sentinels optimization problem is necessary.

The main limitation of the proposed model for solved packing problems relies in the complexity of the continuous optimization problem. Basically, this is a global optimization problem with many local-nonglobal minimizers. General and specific novel strategies for global optimization must be useful for improving the efficiency of the Sentinels approach.

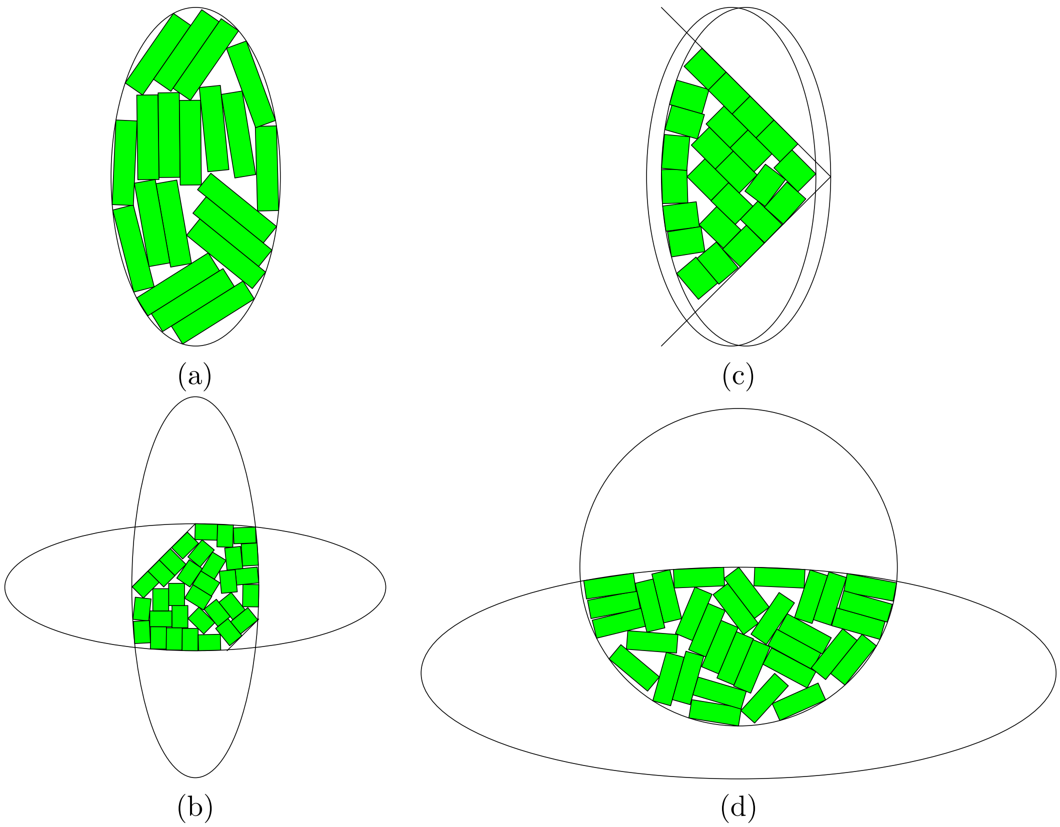

Figure 9: Linear constraints and ellipses (Problems 7 to 10).

Problem	Region S	Packed objects	
		Dimensions	Number
1	$g_1(x_1,x_2) = -x_1$ $g_2(x_1,x_2) = -x_2$ $g_3(x_1,x_2) = -x_1 - x_2 + 3$ $g_4(x_1,x_2) = x_1^2 + x_2^2 - 100$	2×1	32
2	$g_1(x_1,x_2) = -7x_1 + 6x_2 - 24$ $g_2(x_1,x_2) = 7x_1 + 6x_2 - 108$ $g_3(x_1,x_2) = (x_1-6)^2 + (x_2-8)^2 - 9$	1.1×0.55	30
3	$g_1(x_1,x_2) = -x_1$ $g_2(x_1,x_2) = x_1 - 8$ $g_3(x_1,x_2) = (x_1-6)^2 + x_2^2 - 81$ $g_4(x_1,x_2) = (x_1-1.7)^2 + (x_2-10)^2 - 81$	2×0.6	38
4	$g_1(x_1,x_2) = x_1^2 - x_2$ $g_2(x_1,x_2) = x_1^2/4 + x_2 - 5$	1×0.4	28
5	$g_1(x_1,x_2) = x_1^2 - x_2$ $g_2(x_1,x_2) = -x_1 + x_2^2 - 6x_2 + 6$ $g_3(x_1,x_2) = x_1 + x_2 - 6$	0.9×0.3	35
6	$g_1(x_1,x_2) = -x_1 + x_2^2 - 6x_2 + 6$ $g_2(x_1,x_2) = x_1 + x_2^2 - 3x_2 - 3/4$	0.9×0.3	31
7	$g_1(x_1,x_2) = (x_1-2)^2/4 + (x_2-4)^2/16 - 1$	2×0.5	20
8	$g_1(x_1,x_2) = (x_1-6)^2/4 + (x_2-6)^2/36 - 1$ $g_2(x_1,x_2) = (x_1-6)^2/36 + (x_2-6)^2/4 - 1$ $g_3(x_1,x_2) = x_1 - x_2 - 3$ $g_4(x_1,x_2) = -x_1 + x_2 - 2$	0.7×0.5	30
9	$g_1(x_1,x_2) = (x_1-3)^2/4 + (x_2-4)^2/16 - 1$ $g_2(x_1,x_2) = (x_1-2.65)^2/4 + (x_2-4)^2/16 - 1$ $g_3(x_1,x_2) = -x_1 + 1$ $g_4(x_1,x_2) = x_1 - x_2 - 1$ $g_5(x_1,x_2) = x_1 + x_2 - 9$	0.8×0.6	23
10	$g_1(x_1,x_2) = (x_1-6)^2/36 + (x_2-6)^2/4 - 1$ $g_2(x_1,x_2) = (x_1-6)^2/9 + (x_2-8)^2/9 - 1$	0.95×0.35	32
11	$g_1(x_1,x_2) = -x_1$ $g_2(x_1,x_2) = x_1 - (2 + \sqrt{2}/2)$ $g_3(x_1,x_2) = -x_2$ $g_4(x_1,x_2) = x_2 - (2 + \sqrt{2}/2)$	1×1	5
12	$g_1(x_1,x_2) = -x_1$ $g_2(x_1,x_2) = x_1 - (3 + \sqrt{2}/2)$ $g_3(x_1,x_2) = -x_2$ $g_4(x_1,x_2) = x_2 - (3 + \sqrt{2}/2)$	1×1	10
13	$g_1(x_1,x_2) = -x_1$ $g_2(x_1,x_2) = x_1 - 3.878$ $g_3(x_1,x_2) = -x_2$ $g_4(x_1,x_2) = x_2 - 3.878$	1×1	11
14	$g_1(x_1,x_2) = -x_1$ $g_2(x_1,x_2) = x_1 - 4.676$ $g_3(x_1,x_2) = -x_2$ $g_4(x_1,x_2) = x_2 - 4.676$	1×1	17
15	$g_1(x_1,x_2) = -x_1$ $g_2(x_1,x_2) = x_1 - (7 + \sqrt{7}/2)$ $g_3(x_1,x_2) = -x_2$ $g_4(x_1,x_2) = x_2 - (7 + \sqrt{7}/2)$	1×1	18

Table 1: Problems and regions. The regions are of the form $\Omega = \{x \in I\!R^2 \mid g_i(x) \leq 0\}$. In Problem 25, region Ω has the form $\Omega = \{x \in I\!R^2 \mid g_i(x) \leq 0\} - \{x \in I\!R^2 \mid \tilde{g}_i(x) \leq 0\}$. In most of the problems, the packed objects are rectangles. When the objects are not rectangles, they are composed by a combination of (overlapped or not overlapped) rectangles of the mentioned dimensions (See pictures).

Problem	Region S	Packed objects	
		Dimensions	Number
16	$g_1(x_1,x_2) = -x_1$ $g_2(x_1,x_2) = x_1 - (3+4\sqrt{2}/3)$ $g_3(x_1,x_2) = -x_2$ $g_4(x_1,x_2) = x_2 - (3+4\sqrt{2}/3)$	1×1	19
17	$g_1(x_1,x_2) = -x_1$ $g_2(x_1,x_2) = x_1 - (7/2+3\sqrt{2}/2)$ $g_3(x_1,x_2) = -x_2$ $g_4(x_1,x_2) = x_2 - (7/2+3\sqrt{2}/2)$	1×1	26
18	$g_1(x_1,x_2) = -x_1$ $g_2(x_1,x_2) = x_1 - 6.621$ $g_3(x_1,x_2) = -x_2$ $g_4(x_1,x_2) = x_2 - 6.621$	1×1	37
19	$g_1(x_1,x_2) = \sqrt{3}x_1 + x_2 - \sqrt{3}(3/2+\sqrt{3})$ $g_2(x_1,x_2) = -\sqrt{3}x_1 + x_2$ $g_3(x_1,x_2) = -x_2$	1×1	27
20	$g_1(x_1,x_2) = \sqrt{3}x_1 + x_2 - \sqrt{3}(2+4/\sqrt{3})$ $g_2(x_1,x_2) = -\sqrt{3}x_1 + x_2$ $g_3(x_1,x_2) = -x_2$	1×1	28
21	$g_1(x_1,x_2) = \sqrt{3}x_1 + x_2 - \sqrt{3}(3+4/\sqrt{3})$ $g_2(x_1,x_2) = -\sqrt{3}x_1 + x_2$ $g_3(x_1,x_2) = -x_2$	1×1	29
22	$g_1(x_1,x_2) = \sqrt{3}x_1 + x_2 - \sqrt{3}(2+2\sqrt{3})$ $g_2(x_1,x_2) = -\sqrt{3}x_1 + x_2$ $g_3(x_1,x_2) = -x_2$	1×1	30
23	$g_1(x_1,x_2) = \sqrt{3}x_1 + x_2 - \sqrt{3}(4+4/\sqrt{3})$ $g_2(x_1,x_2) = -\sqrt{3}x_1 + x_2$ $g_3(x_1,x_2) = -x_2$	1×1	31
24	$g_1(x_1,x_2) = -x_1$ $g_2(x_1,x_2) = x_1 - 23$ $g_3(x_1,x_2) = -x_2$ $g_4(x_1,x_2) = x_2 - 21$	6×5	16
25	$g_1(x_1,x_2) = -x_1$ $g_2(x_1,x_2) = x_1 - 10$ $g_3(x_1,x_2) = -x_2$ $g_4(x_1,x_2) = x_2 - 8$	2×1	40
26	$g_1(x_1,x_2) = -x_1$ $g_2(x_1,x_2) = x_1 - 10$ $g_3(x_1,x_2) = -x_2$ $g_4(x_1,x_2) = x_2 - 8$	2×1	34 + 6 fixed
27	$g_1(x_1,x_2) = -x_1$ $g_2(x_1,x_2) = x_1 - 10$ $g_3(x_1,x_2) = -x_2$ $g_4(x_1,x_2) = x_2 - 8$	2×1	34 + 6 fixed
28	$g_1(x_1,x_2) = -x_1$ $g_2(x_1,x_2) = x_1 - 10$ $g_3(x_1,x_2) = -x_2$ $g_4(x_1,x_2) = x_2 - 8$	2×1	34 + 4 fixed
29	$g_1(x_1,x_2) = -x_1 + x_2 - 6$ $g_2(x_1,x_2) = x_1 - x_2 - 6$ $g_3(x_1,x_2) = -x_1 - x_2 + 6$ $g_4(x_1,x_2) = x_1 + x_2 - 18$ $g_5(x_1,x_2) = -x_1 + 1$ $g_6(x_1,x_2) = x_1 - 11$ $g_7(x_1,x_2) = -x_2 + 1$ $g_8(x_1,x_2) = x_2 - 11$	2×1	28 + 2 fixed
30	$g_1(x_1,x_2) = (x_1-6)^2/36 + (x_2-6)^2/4 - 1$ $g_2(x_1,x_2) = (x_1-6)^2/9 + (x_2-6)^2/9 - 1$	0.95×0.35	14

Table 2: Problems and regions (continuation).

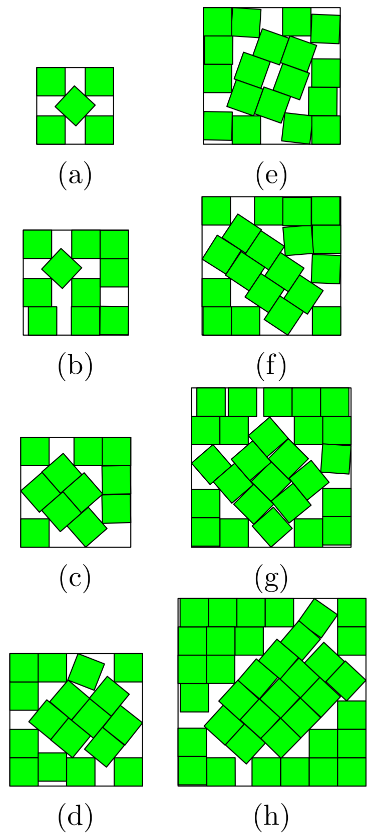

Figure 10: Squares into squares (Problems 11 to 18).

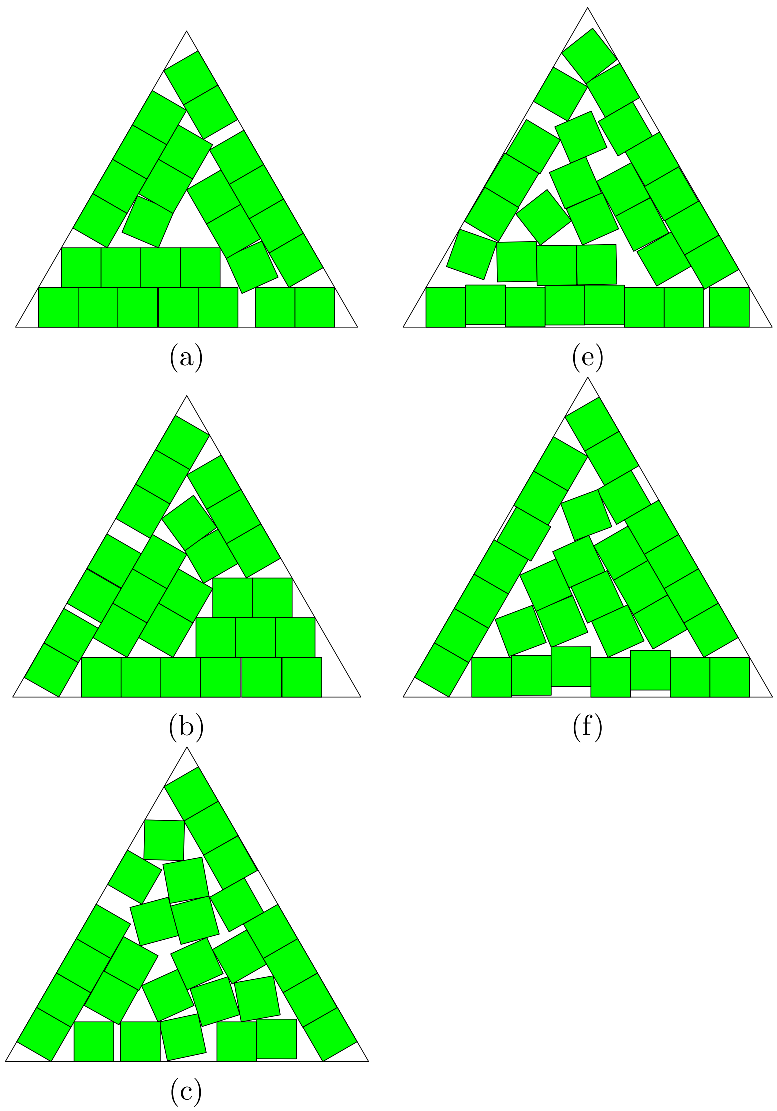

Figure 11: Squares into triangles (Problems 19 to 23).

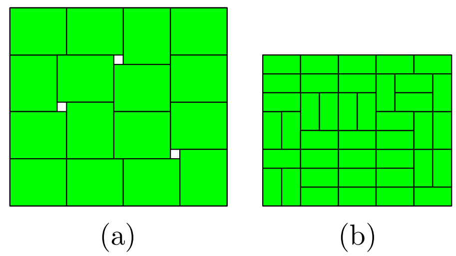

Figure 12: A non-guillotine and a guillotine patern (Problems 24 and 25).

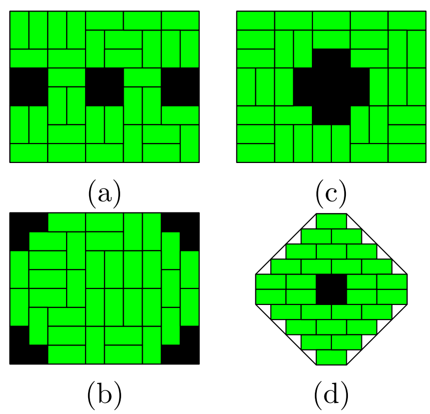

Figure 13: Forbidden regions for special pallet configurations (Problems 26 to 29).

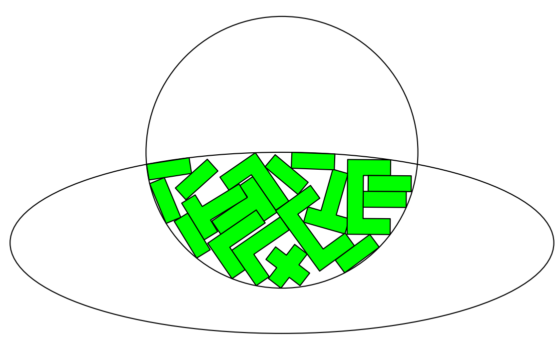

Figure 14: Packing of nonrectangular objects (Problem 30).

6 Appendix: Proofs of Section 3

Here we collect the technical proofs and theorems stated in Section 3. The results are proved in the order that they were stated.

Proof of Lemma 1. The proof is by induction. To start the induction, notice that any polygon with angles bigger than or equal to $\pi/2$ with four sides must be a rectangle and the polygons with five sides with this property are convex too. To apply the induction step for polygons with six or more sides, we show that any non convex polygon with internal angles bigger than or equal to $\pi/2$ and six or more sides can be splitted into simpler parts. The parts are simpler in the sense that they have fewer vertices than the original polygon, or have fewer reflex vertices or have more internal angles equal to $\pi/2$, in this order. To prove this claim we analyze the possibilities described in in the next seven figures which cover all possible cases with a reflex (or nonconvex) vertex. The idea of the analysis is to let a scan line rotate around the reflex vertex and check all the possible events that may happen as the scan line rotates. We start with two preliminary cases and then focus at the scan line. The scan line starts its movement connecting the point a to the reflex vertex p_k so that $ap_k \perp p_kp_{k+1}$. It rotates until it reaches the point b, such that $bp_k \perp p_kp_{k-1}$. Let us then look at the several cases.

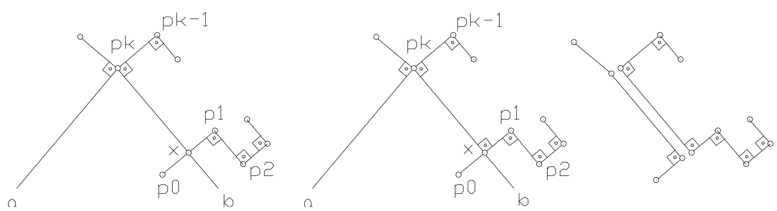

Figure 15: The angles $\widehat{p}_1$, $\widehat{p}_2$, $\ldots \widehat{p}_{k-1}$ are $\pi/2$, p_0p_1 crosses p_kb at x and x is visible from p_k.

In the first case all the angles $\widehat{p}_1$, $\widehat{p}_2$, $\ldots \widehat{p}_{k-1}$ are equal to $\pi/2$, p_0p_1 crosses p_kb at x and x is visible from p_k. In this case the sides p_jp_{j+1} for $j = 0, \ldots, k$ are either orthogonal or parallel. In particular, p_0p_1 must be orthogonal to p_kb and parallel to $p_{k-1}p_k$. Thus, we can split P along the line xp_k as described in Figure 15, obtaining two polygons with fewer vertices than P.

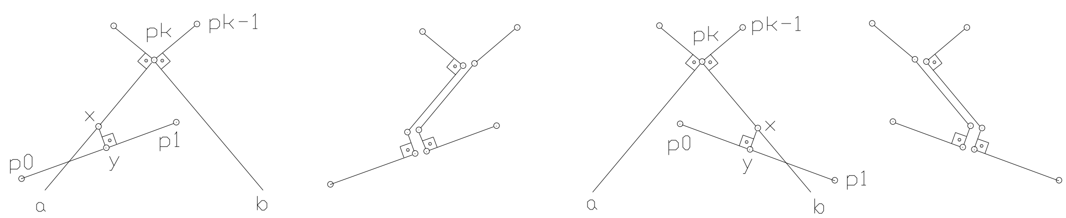

Figure 16: The side p_0p_1 makes an acute angle with ap_k and the symmetric case.

In the second case p_0p_1 makes an acute angle with ap_k. More precisely, p_0p_1 intercepts ap_k at a point x and there exists $y \in p_0p_1$ such that $xy \perp p_0p_1$ and the sides of P do not cut the relative interior of p_kx and xy. This case also considers the analog situation obtained by reflecting things along the y axis, as exposed in Figure 16. In this case we can split P along the line p_kxy (see Figure 16). On the right hand side we get a polygon with at least as many vertices as P but with one reflex vertex less. The polygon on the left hand side may have at most as many vertices as P and at most the same number of reflex vertices. In fact, in order to get the polygon on the left we added two vertices, x and y and removed at least two, p_{k-1} and p_1. If we removed any other vertex then we have reduced P. Otherwise, the polygon on the left has as many vertices as P. If the angles $\widehat{p}_1$ and $\widehat{p}_{k-1}$ are $\pi/2$ then we are in Case 1. Otherwise, one of them is not $\pi/2$ and we removed at least one internal angle different from $\pi/2$, on top of $\widehat{p}_k$. Since we inserted only one internal angle different from $\pi/2$, the number of internal angles different from $\pi/2$ decreases by one and we are done with Case 2.

Now we start to track the scan line. In the third case it does not hit any vertex visible from p_k as it moves. In this case there must be a side p_0p_1 hiding the rest of P from p_k, as in Figure 17 and the triangle xp_ky must have one of the angles $p_k\widehat{x}y$ or $p_k\widehat{y}x$ smaller than $\pi/2$. This reduces the third case to the second.

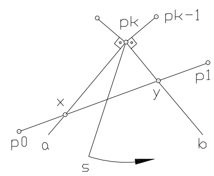

Figure 17: The scan line s does not hit vertices visible from p_k as it rotates from a to b.

In the fourth case the scan line hits a reflex vertex u visible from p_k and with neighbors x and v on the same side of s. In this case we look at the angle $p_k\widehat{u}v$. If it is smaller than $\pi/2$ then we add point q close to u, as described in Figure 18, and split P along the line p_kqux. If the angle $p_k\widehat{u}v$ is bigger than or equal to $\pi/2$ we split P along the line p_kux. In both cases we get parts with fewer vertices than P.

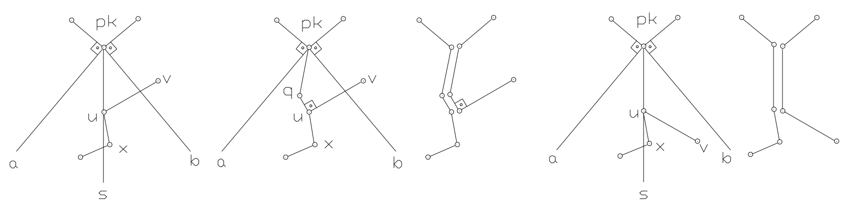

Figure 18: The scan line s hits a reflex vertex u with both neighbors on the same side of s.

In the fifth case, s gets to a vertex u visible from p_k at which the internal angle is $\pi/2$. In this case we add a point q in the segment p_ku, close to u, and take the projections of q on the sides neighboring u, as in Figure 19. We then split P in simpler parts, as described in this Figure.

In the sixth case, s passes through only one vertex u visible from p_k as it travels from a to b. If the internal angle at u were $\pi/2$ then we would be in the last case. If any of the angles between tu and ap_k or uv and bp_k were less than $\pi/2$ (see Figure 20) then we would be in Case 2. Therefore we can assume that the internal angle at u is bigger than $\pi/2$ and that Figure 20

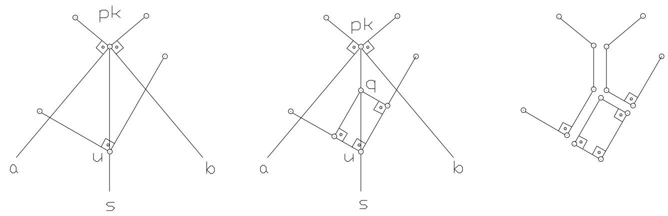

Figure 19: The scan line s gets to a vertex u with internal angle equal to $\pi/2$.

is accurate in the sense that the points x and y are either in the correct side of the segments ap_k and bp_k or over them, if the angles were exactly $\pi/2$. We then move x and y to their new positions indicated in Figure 20 in order to avoid degeneracies, like having t or v on ap_k or bp_k, and to make xy orthogonal to up_k. (This can always be achieved by taking x and y very close to u.) Next we split P as indicated in Figure 20, obtaining simpler parts because

1. The bottom part is convex

2. Either we are in Case 1 or the left part L has at most as many vertices as P. If L has the same number of vertices as P then it has one more right angle than P. In fact, we added three vertices to build L (z, x and w) and removed at least three others (u, v and p_{k-1}.) Thus L has at most as many vertices as P. In the case that L and P have the same number of vertices, notice that P has $n_L + n_R + 2$ internal angles different from $\pi/2$, where n_L is the number of internal angles different from $\pi/2$ among the vertices from p_{k+1} to t and n_R is the number of internal angles different from $\pi/2$ among the vertices from v to p_{k-1}. The "2" is due to u and p_k, at which the internal angle is also different from $\pi/2$. L, on the other hand, has $n_L + 2$ internal angles different from $\pi/2$, the old n_L ones plus the one at p_k and the one at x. If n_R where zero then we would be in Case 1. Otherwise $n_L + 2 < n_L + n_R + 2$ and L has fewer angles different from $\pi/2$ than P, as we have claimed.

3. The right part is analogous to the left one.

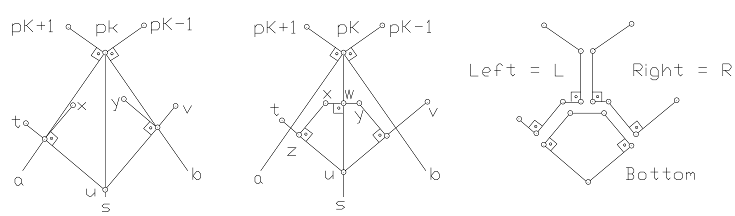

Figure 20: The scan line s passes through only one vertex u as it travels from a to b.

Finally, we have the seventh and last case, when the scan line passes through two or more vertices as it moves from a to b. If one of such vertices were reflex we would be in Case four. Otherwise, the whole segment uv would be visible from p_k and we could take x and y as described in Figure 21. We could then split P along the line $p_k yxv$, as illustrated in this figure. This would lead to parts with fewer vertices than P, because we would insert two vertices (x and y) and, as the reader can verify in the accurate Figure 21, we would remove more than two vertices during the construction of each of the parts. This completes the proof of Lemma 1 •

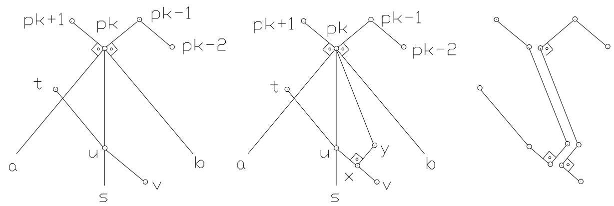

Figure 21: The scan line s passes through at least two vertices u and v as it moves from a to b.

Proof of Lemma 2. Let D be a displacement such that $A_k \cap D(A_j) \neq \emptyset$ for some $i \neq j$. Take $a \in A_i \cap D(A_j)$. By the way A_i and A_j are decomposed according to the hypothesis on the decomposition of the A's, there is i_k and i_j such that $c \in A_{ki_k} \cup D(A_{ji_j})$ and, by the hypothesis on the S_{ij}'s, either $A_{ki_k} \cap D(S_{ji_j}) \neq \emptyset$ or $S_{ki_k} \cap D(A_{ji_j}) \neq \emptyset$. Thus, we either have $A_k \cap D(S_j) \neq \emptyset$ or $S_k \cap D(A_j) \neq \emptyset$. This shows that the S_i's are sentinels for the A_i's as claimed in Lemma 2 •

Proof of Lemma 3. If $P = P_i$ is one of the polygons in the hypothesis and p is one its vertices then there exists a straight line r and points x and y as described in Figure 22, that is P is contained in the triangle xpy and the segment xy is parallel to r.

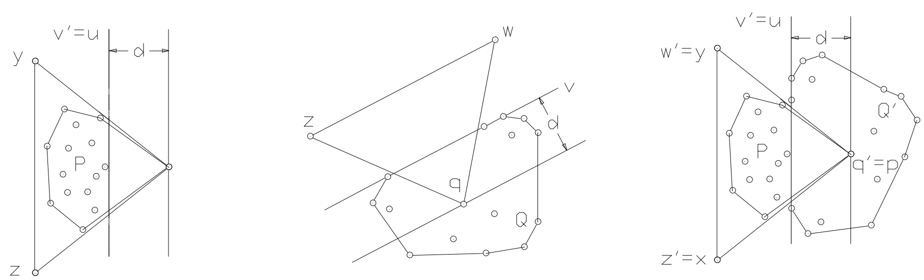

Figure 22: If the vertex p of P is not a sentinel then we can move it into Q.

Take another polygon Q in the family P_i, $q \in Q$ and a small number d such that the Figure 22 is accurate, that is,

1. The distance of any sentinel of P different from p to r is bigger than d.
2. The point q is at a distance d from the side of border of Q contained in the straight line v. The triangle zqw, obtained by displacing the triangle xpy so that the side zw is parallel to v, does not contain sentinels of Q.

Consider now the displacement of Q described in Figure 22: rotate Q so that v becomes parallel to u and translate it until q and p coincide. By the way d was chosen, the intersection of Q' and P contains no sentinel of Q. It also does not contain any sentinel of P other than, possibly, p. Since this intersection is not empty it must contain at least one sentinel and, thus, p must be a sentinel and this proof is complete •

Proof of Theorem 2. Suppose that there exists a point p in the intersection of the interior of the polygons $P = P_i$ and $Q = D(P_j)$, for some displacement operator D. Since p is in the interior of Q, the condition 4 on the hypothesis implies that there exists and internal sentinel s of Q such that the segment pq is contained in the interior of Q. If this segment contains a vertex v of P then we are done because in this case $v \in S(P_i) \cap D(P_j)$. If q is in the interior of P then we will be done too, because in this case $q \in P_i \cap D(S_j)$. Since p is in the interior of P and q is not, the segment pq must cross the border of P at a point r, which is in the interior of Q. By item 3 in the hypothesis, there are sentinels s and s' on a side $p_j p_{j+1}$ of P such that $r \in ss'$ and $\|s - s'\| \leq \delta$. Notice that if either s or s' are in the interior of Q then we are done. Otherwise, we must have sides $q_a q_b$ and $q'_a q'_b$ of Q separating s and s' from r. We may also assume that p is very close to r, so that $\|r - p\| \leq \min\{\|r - u\|, \|r - v\|\}$. The last arguments reduce the proof to the case in which the Figure 23 is accurate.

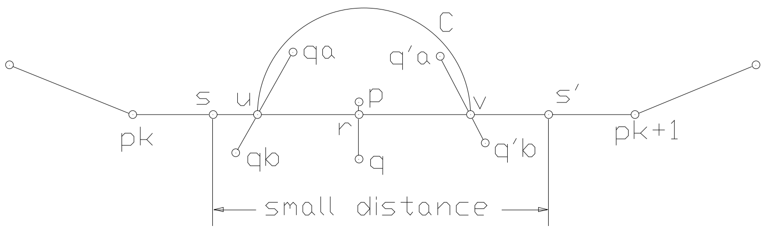

Figure 23: The point p is in the interior of P_i and $D(P_j)$, $q \in D(S_j)$ and $4pq$ intercepts P at $r \in ss' \subset p_k p_{k+1}$, which is very close to p. The sides $q_a q_b$ and $q'_a q'_b$ of Q separate r from s and s', respectively, and q_b,q'_b and q are on the same side of the straight line containing $p_k p_{k+1}$.

Now, notice that $\|u - v\| \leq \delta$, because $\|s - s'\| \leq \delta$. Thus, by Condition 1 in the hypothesis, uv cannot split Q. This implies that $q_a q_b$ and $q'_b q'_b$ are consecutive sides of Q and we have two possibilities: either $q_a = q'_a$ or $q_b = q'_b$. However, $q_b = q'_b$ is not possible because of the last condition on the hypothesis. In fact, if q_b were equal to q'_b then q would be in the interior of the triangle $q_a q_b q'_a$, which is formed by three consecutive vertices of Q, contradicting the item 5 in the hypothesis. Thus we must have $q_a = q'_a$. Since the internal angle $q_b \widehat{q}_a q'_b$ of Q is bigger than or equal to $\pi/2$, q_a is contained in the circle with diameter uv, In fact, since q_a and q are in opposite sides of $p_k p_{k+1}$, q_a belongs to the semicircle C in Figure 23. Therefore, $\|q_a - p\| \leq \delta$. Notice that the neighbor sides of $p_k p_{k+1}$ in P intersect C at most at p_k and p_{k+1}, because the internal angles of P at p_k and p_{k+1} are bigger than or equal to $\pi/2$. As a consequence the border of P cannot intersect the segment $q_a p$. In fact, if the border of P did intercept $q_a p$ at a point t then, by the convexity of the semicircle C, tr would be contained in C and would have length $\|t - r\| \leq \delta$. Moreover, t and r would be in nonconsecutive sides of P, because the neighbor sides of $p_k p_{k+1}$ do not touch C in points other than p_k and p_{k+1}. Thus tr would split P and have length $\leq \delta$, what contradicts the item 1 in the hypothesis. Therefore, since $q_a p$ does not touch the border of P and p belongs to the interior of P, q_a is also in the interior of P. Finally, the item 2 in the hypothesis implies that q_a, which is a vertex of $Q = D(P_j)$, belongs to $D(S_j)$. This shows that $P_i \cap D(S_j) \neq \emptyset$ and completes the proof •

Proof of Lemma 5. This lemma is proved by Figure 24. Notice that the superposition of R and R' has a non empty interior (hatched area) which contains no sentinels. The only way to avoid this construction is to have sentinels in the relative interior of the segment ab •

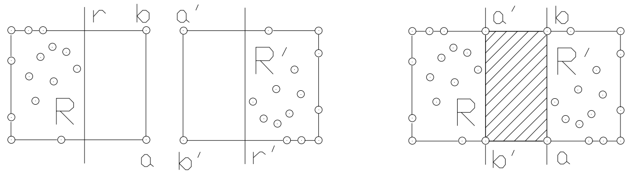

Figure 24: R has all its sentinels other than a and b to the left of the line r. R' is a copy of R rotated by π.

Proof of Lemma 6. To simplify the notation, we refer to the interior R_λ simply as R. Let C_ν be the square defined by

$$C_\nu = \{(x,y) \in I\!R^2 \text{ such that } \nu < x < \nu + 2 \text{ and } |y| \le 1\}, \tag{32}$$

for $-\lambda \le \nu \le \lambda - 2$. We claim that if S is a sentinel set of R then there is an element of S in C_ν. In fact, if we rotate R by $\pi/2$ around the center of C_ν we get the rectangle R' described in Figure 25. More generally, from now on we will use A' to indicate the displaced copy of the set A obtained by the same process used to get R' from R.

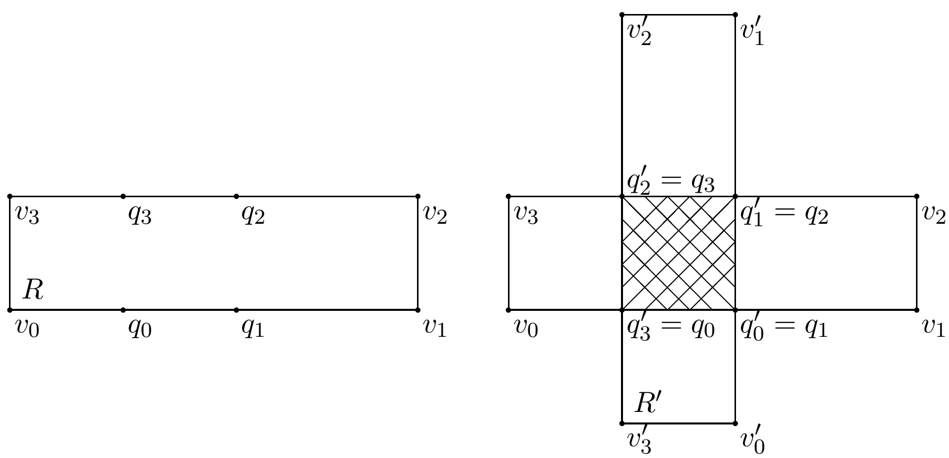

Figure 25: If the segments q_0q_1 and q_3q_2 are too long then we can put a rotated copy of R between them.

Since $R \cap R' \neq \emptyset$ and S is a sentinel set we either have $S \cap R' \neq \emptyset$ or $S' \cap R \neq \emptyset$. In the first case, since $S \subset \overline{R}$ and $\overline{R} \cap R' = C_\nu$, we have

$$S \cap R' = S \cap (\overline{R} \cap R') = S \cap C_\nu \neq \emptyset.$$

In the second case, decompose S as $S = X \cup Y$, where $X = S \cap C_\nu$ and $Y = S \cap (\overline{R} - C_\nu)$. Since Y is a subset of $(\overline{R} - C_\nu)$,

$$Y' \cap R \subset (\overline{R} - C_\nu)' \cap R = \emptyset.$$

Therefore, in the second case

$$S' \cap R = (X' \cap R) \cup (Y' \cup R) = X' \cap R \neq \emptyset.$$

This implies that $X = S \cap C_\nu$ is not empty and we have shown that our claim that $S \cap C_\nu \neq \emptyset$ is valid. As a consequence of the claim, each one of the $\lfloor \lambda \rfloor$ disjoint sets $C^{2i-\lambda}$, for $i = 0, 1, \dots, \lfloor \lambda \rfloor - 1$, contains a sentinel. Adding the three sentinels on the right side of R given by lemmas 3 and 5 and the three on the left side we get a total of at least $3 + 3 + \lfloor \lambda \rfloor$ sentinels and lemma 6 is proved •

Proof of Theorem 3. Our proof is based on the analysis of the "dual" sets associated with each rotation angle θ described in the last section. Along the proof λ will be constant and thus we drop it from R, S and T. According to the discussion in the last section, in order to prove the present theorem it is enough to show that

$$\mathcal{R}_\theta = \mathcal{R}_\theta(S) = \mathcal{R}_\theta(T),$$

for

$$\begin{aligned} \mathcal{R}_\theta &= \mathcal{D}_\theta(R, R), & (33) \\ \mathcal{R}_\theta(A) &= \mathcal{D}_\theta(A, R) \cup \mathcal{D}_\theta(R, A). & (34) \end{aligned}$$

The dependency of $\mathcal{R}_\theta$ on θ is described in Figure 26. When $0 \leq \theta < \pi$, the arrows indicate symmetry axis with directions $(1 + c, s)$ and $(-s, 1 + c)$, for

$$\begin{aligned} c &= \cos\theta, \\ s &= \sin\theta. \end{aligned}$$

R is the horizontal rectangle and the inclined rectangle is rotated by θ, without translation.

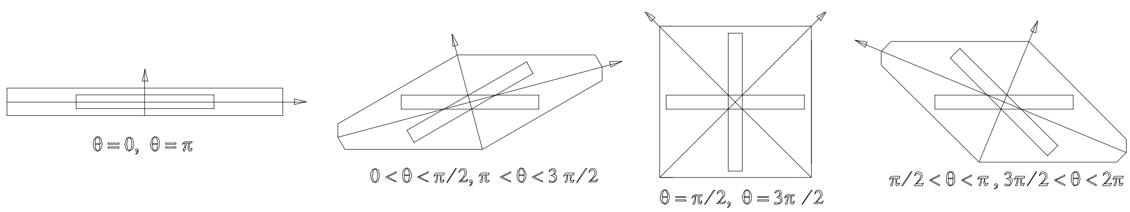

Figure 26: The dual sets $\mathcal{R}_\theta$ for different values of θ.

As Figure 26 suggests, there are many cases to be analyzed and our strategy will be to exploit the symmetries of $\mathcal{R}_\theta$, R,S and T to try to minimize the number of cases in the analysis. Unfortunately, even after some reductions, our approach still requires a lot of cases and we could not find a more concise way to prove this theorem. We leave the analysis of the myriad of particular cases to lemmas that will be proved after this proof is complete and present here a higher level view. In order to formalize the symmetries mentioned above, we will use the sets

$$\begin{aligned} Q_\theta &= \{(x, y) \in \mathcal{R}_\theta \text{ such that } (1 + c)x + sy \geq 0 \text{ and } (1 + c)y - sx \geq 0\} & (35) \\ \tilde{Q}_\theta &= \{(x, y) \in \mathcal{R}_\theta \text{ such that } (1 + c)x + sy \geq 0 \text{ and } (1 + c)y - sx \leq 0\}. & (36) \end{aligned}$$

These sets correspond to the first and fourth quadrants for the axis in Figure 26 and the reader can verify that they decompose $\mathcal{R}_\theta$ in the sense that

$$\mathcal{R}_\theta = Q_\theta \cup \tilde{Q}_\theta \cup -Q_\theta \cup -\tilde{Q}_\theta. \tag{37}$$

We will be mainly concerned with Q_θ for $\theta \in [0, \pi/2]$, which is characterized by the next lemma

Lemma 7 *If $\theta \in [0, \pi/2]$ then any $(x, y)^t \in Q_\theta$ satisfies the following inequalities:*

$$\begin{aligned}
(1+c)x + sy &\geq 0, && (38)\\
(1+c)y - sx &\geq 0, && (39)\\
y &< 1 + s\lambda + c, && (40)\\
cx + sy &< (1+c)\lambda + s, && (41)\\
y &\geq 0, && (42)\\
cx + sy &\geq 0. && (43)
\end{aligned}$$

The last lemma is the main ingredient to prove next three lemmas, which show that Q_θ is covered by $\mathcal{R}_\theta(S)$ and $\mathcal{R}_\theta(T)$ for all $\theta \in [0, \pi/2]$:

Lemma 8 *$\mathcal{R}_0(S) \supset Q_0$ and $\mathcal{R}_0(T) \supset Q_0$.*

Lemma 9 *$\mathcal{R}_{\pi/2}(S) \supset Q_{\pi/2}$ and $\mathcal{R}_{\pi/2}(T) \supset Q_{\pi/2}$.*

Lemma 10 *If $0 < \theta < \pi/2$ then $\mathcal{R}_\theta(S) \supset Q_\theta$ and $\mathcal{R}_\theta(T) \supset Q_\theta$.*

The next step is to extend this result for the remaining quadrants and for all θ using symmetries related to the reflection on the x axis, which is given by

$$F = \begin{pmatrix} -1 & 0 \\ 0 & 1 \end{pmatrix}, \tag{44}$$

and are listed in the following lemmas:

Lemma 11 *If A is a subset of $\overline{R}$ then*

$$\mathcal{R}_\theta(-A) = -\mathcal{R}_\theta(A). \tag{45}$$

Lemma 12 *If A is a subset of $\overline{R}$ and $-\pi < \theta < \pi$ then*

$$(\mathcal{R}_\theta(A) \supset Q_\theta) \Rightarrow \left(\mathcal{R}_\theta(FA) \supset \tilde{Q}_\theta\right). \tag{46}$$

Lemma 13 *If A is a subset of $\overline{R}$ then*

$$(\mathcal{R}_\theta(A) \supset \mathcal{R}_\theta) \Rightarrow (\mathcal{R}_{-\theta}(FA) \supset \mathcal{R}_{-\theta}). \tag{47}$$

Lemma 14 *If A is a subset of $\overline{R}$ such that $-A = A$ then*

$$(\mathcal{R}_\theta(A) \supset \mathcal{R}_\theta) \Rightarrow (\mathcal{R}_{\theta+\pi}(A) \supset \mathcal{R}_{\theta+\pi}). \tag{48}$$

Combining lemmas 8 – 12 we deduce that for $\theta \in [0, \pi/2]$,

$$(\mathcal{R}_\theta(T) \supset Q_\theta) \Rightarrow \left(\mathcal{R}_\theta(FT) \supset \tilde{Q}_\theta\right) \Rightarrow \left(\mathcal{R}_\theta(S) \supset \tilde{Q}_\theta\right).$$

Therefore, if $\theta \in [0, \pi/2]$, lemmas 8, 9 and 10 lead to

$$\mathcal{R}_\theta(S) \supset Q_\theta \cup \tilde{Q}_\theta.$$

Thus, the identity $S = -S$, lemma 11 and (37) imply

$$\mathcal{R}_\theta(S) \supset Q_\theta \cup \tilde{Q}_\theta \cup -Q_\theta \cup -\tilde{Q}_\theta = \mathcal{R}_\theta$$

if $\theta \in [0, \pi/2]$. Analogously, $\mathcal{R}_\theta(T) \supset \mathcal{R}_\theta$ if $\theta \in [0, \pi/2]$. We then use Lemma 13, the identities $FS = T$, $FT = S$ and Lemma 13 to extend these results to $[-\pi/2, \pi/2]$. Finally, we use lemma 14 to extend the result to $[-\pi/2, 3\pi/2]$. This last interval has length 2π and every angle θ can be reduced to it and the proof of Theorem 3 is complete •

Proof of Lemma 7. The term $Q_\theta \subset \mathcal{R}_\theta$ is an abbreviation for $\mathcal{D}_\theta(R_\lambda, R_\lambda)$, which was defined in 21, where R_λ is the rectangle with vertices $(\pm\lambda, \pm 1)^t$. Thus, $d = (x, y)^t$ belongs to $\mathcal{D}_\theta$ if and only if

$$\begin{aligned} x &= a + cp - sq, & (49)\\ y &= b + sp + cq & (50) \end{aligned}$$

with

$$\begin{aligned} -\lambda < a, p < \lambda, && (51)\\ -1 < b, q < 1. && (52) \end{aligned}$$

The combination $c(49) + s(50)$ leads to

$$cx + sy = ca + sb + p.$$

This equation, the bounds (50), (51), (52), the definition of Q_θ in (35) and straightforward algebra imply the bounds (38) – (41). Multiplying (38) by s, which is nonnegative since $\theta \in [0, \pi/2]$, multiplying (39) by $1 + c$ and adding, we obtain (42). Finally, (38) and $c \neq -1$ imply

$$x \geq \frac{-sy}{1 + c}$$

and

$$cx + sy \geq \frac{c(-sy)}{1 + c} + sy = \frac{sy}{1 + c} \geq 0.$$

This verifies the bound (43) and completes the proof of Lemma 7 •

Proof of Lemma 8. This lemma treats the case $\theta = 0$. In this particular case $c = 1$ and $s = 0$ and the bounds (38) – (43) on the coordinates x, y of $d \in Q_0$ imply

$$\begin{aligned} 0 &\leq x < 2\lambda, & (53)\\ 0 &\leq y < 2. & (54) \end{aligned}$$

The next table explains how to obtain $s \in S$, $t \in T$ and r_s, r_t in the interior of R such that $d = r_s + H_0 s$ and $d = r_t + H_0 t$.

	$x = 0$	$0 < x < 2\lambda$
$y = 0$	$r_s = r_t = -s = -t = (1 - 2\delta, 0)^t$	$r_s = r_t = (x - \lambda, 0)^t, s = t = (\lambda, 0)^t$
$0 < y < 2$	$r_s = (\delta - \lambda, y - 1)^t, s = (\lambda - \delta, 1)^t$ $r_t = (\lambda - \delta, y - 1)^t, t = (\delta - \lambda, 1)^t$	$r_s = s_t = (x - \lambda, y - 1)^t$ $s = t = (\lambda, 1)^t$

The reader can use the bounds (53), (54) and $\delta < 2\lambda$ to verify that the r_s, r_t, s and t above are valid and this proof is complete •

In the next proof we use the following lemma.

Lemma 15 *If $0 < s \leq 1$ and $|l| < s(\lambda - 2\delta) + 1$ then there exists an integer $k \geq 2$ for which $(k\delta - \lambda, 0) \in S \cap T$ and such that $|l - s(k\delta - \lambda)| < 1$.*

Proof of Lemma 9. If $\theta = \pi/2$ then $c = 0$ and $s = 1$ and the bounds (38) – (42) on the coordinates x, y of $d \in Q_{\pi/2}$ become

$$
\begin{aligned}
x + y &\geq 0, && (55)\\
y - x &\geq 0, && (56)\\
0 \leq y &< 1 + \lambda. && (57)
\end{aligned}
$$

We proceed by looking at 8 cases below, which cover all possibilities for x and y:

$$
\begin{aligned}
x &< 1 - \lambda && (58)\\
x &> \lambda - 1 && (59)\\
|x| \leq \lambda - 1, \quad \text{and} \quad y &\leq \lambda - \delta - 1 && (60)\\
|x| \leq \lambda - 1 \quad \text{and} \quad \lambda - \delta - 1 < y &< \lambda - 1 && (61)\\
x = 1 - \lambda, \quad \text{and} \quad y &= \lambda - 1 && (62)\\
|x| < \lambda - 1, \quad \text{and} \quad y &= \lambda - 1 && (63)\\
x = \lambda - 1, \quad \text{and} \quad y &= \lambda - 1 && (64)\\
|x| \leq \lambda - 1, \quad \text{and} \quad y &> \lambda - 1 && (65)
\end{aligned}
$$

For each case we show that the corresponding $d = (x, y)^t$ belongs to $\mathcal{D}_{\pi/2}(S) \cap \mathcal{D}_{\pi/2}(T)$. We prove that by providing $r \in R$, $s \in S$ and $t \in T$ such that $d = (x, y)^t = s + H_{\pi/2} r$ and $d = t + H_{\pi/2} r$ or $r' \in R$, $s' \in S$ and $t' \in T$ such that $d = r' + H_{\pi/2} s'$ and $d = r' + H_{\pi/2} t'$. Here is how the cases are analyzed:

Case (58): Notice that (55) and (57) imply $x > -1 - \lambda$ and $-(x + \lambda) < 1$ and, in this case, this implies $|x + \lambda| < 1$. Since $y \geq 0$, (57) implies $-\lambda \leq -1 < y - 1 < \lambda$ and we can take $s = t = (-\lambda, 1)^t$ and $r = (y - 1, -x - \lambda)^t$.

Case (59): Notice that (56) and (57) imply $x < \lambda + 1$ and in the present case we obtain $|\lambda - x| < 1$. Since $y \geq 0$, (57) implies $-\lambda < -1 \leq y - 1 < \lambda$ and we can take $r = (y - 1, \lambda - x)^t$ and $s = t = (\lambda, 1)$.

Case (60): Since $\delta < 2$, in the present case (60) leads to

$$0 \le y \le \lambda - 2\delta + 1 + (\delta - 2) < (\lambda - 2\delta) + 1.$$

We can then apply lemma 15 with $l = y$ and $s = 1$ and obtain k such that $s' = t' = (k\delta - \lambda, 0)^t \in S \cap T$ and $|y - (k\delta - \lambda)| < 1$. Moreover, in this case (60) implies $|x| \le \lambda - 1 < \lambda$ and we can take $r' = (x, y - (k\delta - \lambda))^t$.

Case (61): In this case, since $\delta < 2$, we have that $y - \lambda + \delta < \delta - 1 < 1$ and $|y - \lambda + \delta| < 1$. Moreover, (55) and (56) imply $|x| < \lambda - 1$ and lead to $|x \pm 1| < \lambda$. The treatments of S and T are analogous but slightly different. For T we take $r' = (x - 1, y - \lambda - \delta)^t$ and $s = (\delta - \lambda, -1)^t$ and for S we take $r' = (x + 1, -\lambda - \delta)^t$ and $s' = (\delta - \lambda, 1)$ and, since $(x \pm 1, y - \lambda - \delta) \in R$ the analysis of this case is complete.

Case (62): Here we treat S and T separately. For S we proceed as in case 63. For T we take $t = (\delta - \lambda, 1)^t$ and $r = (\lambda - 2, \delta - 1)^t$, which are valid because $0 < \delta < 2 \Rightarrow |\delta - 1| < 1$ and $\lambda > 1 \Rightarrow |\lambda - 2| < \lambda$.

Case (63): For S we take $s' = (\lambda - \delta, 1)^t$ and $r' = (x + 1, \delta - 1)^t$, which are valid because $0 < \delta < 2 \Rightarrow |\delta - 1| < 1$ and in this case (63) implies $|x + 1| < \lambda$. For T we take $t' = (\lambda - \delta, -1)^t$ and $r' = (x - 1, \delta - 1)^t$, which are valid because $0 < \delta < 2 \Rightarrow |1 - \delta| < 1$ and in this case (63) implies $|x - 1| < \lambda$.

Case (64): For S we take $s = (\lambda - \delta, 1)^t$ and $r = (\lambda - 2, 1 - \delta)^t$, which are valid because $0 < \delta < 2 \Rightarrow |1 - \delta| < 1$ and $\lambda > 1 \Rightarrow |\lambda - 2| < \lambda$. For T we proceed as in case 63.

Case (65): In this case(57) imply that $r' = (x, y - \lambda)^t \in R$ and $s' = t' = (\lambda, 0)^t$ are valid.

We have covered all the possibilities and the proof of Lemma 9 is complete •

Proof of Lemma 10. The condition $\theta \in (0, \pi/2)$ is part of the hypothesis of this lemma in order to guarantee that $0 < c, s < 1$. The reader should always keep this in mind while working with the inequalities in this proof. The proof of Lemma 10 is based on the following sequence of lemmas, the proofs of which will be postponed.

Lemma 16 *If $0 < \theta < \pi/2$ then $\mathcal{D}_\theta(S) \cap \mathcal{D}_\theta(T)$ contains the intersection of Q_θ with the half plane*

$$cy - sx < 1 + c - s\lambda. \tag{66}$$

Lemma 17 *If $0 < \theta < \pi/2$ then $\mathcal{D}_\theta(S) \cap \mathcal{D}_\theta(T)$ contains the intersection of Q_θ with the half plane*

$$y > s\lambda + c - 1. \tag{67}$$

Lemma 18 *If $0 < \theta < \pi/2$ then $\mathcal{D}_\theta(S) \cap \mathcal{D}_\theta(T)$ contains the intersection of Q_θ with the half plane*

$$y > s\lambda - 1. \tag{68}$$

Lemma 19 *If $0 < \theta < \pi/2$ then $\mathcal{D}_\theta(S)$ contains the intersection of Q_θ with the half plane*

$$y > s(\lambda - \delta) + c - 1. \tag{69}$$

Lemma 20 *If $0 < \theta < \pi/2$ then $\mathcal{D}_\theta(S)$ contains the intersection of Q_θ with the half plane*

$$cy - sx \leq -s(\lambda - 2\delta) - 1. \tag{70}$$

Lemma 21 *If $0 < \theta < \pi/2$ then $\mathcal{D}_\theta(S)$ contains the intersection of Q_θ with the half plane*

$$cy - sx \geq s(\lambda - 2\delta) + 1. \tag{71}$$

Lemma 22 *If $0 < \theta < \pi/2$ then $\mathcal{D}_\theta(T)$ contains the intersection of Q_θ with the half plane*

$$cy - sx > s(\lambda - \delta) + c - 1. \tag{72}$$

Lemma 23 *If $0 < \theta < \pi/2$ then $\mathcal{D}_\theta(T)$ contains the intersection of Q_θ with the half plane*

$$y \geq s(\lambda - \delta) + 1 - c. \tag{73}$$

Lemma 24 *If $0 < \theta < \pi/2$ then $\mathcal{D}_\theta(T)$ contains the intersection of Q_θ with the half plane*

$$cy - sx \leq -s(\lambda - 2\delta) - 1. \tag{74}$$

Lemma 25 *If $0 < \theta < \pi/2$ then $\mathcal{D}_\theta(T)$ contains the intersection of Q_θ with the half plane*

$$cy - sx \geq s(\lambda - 2\delta) + 1. \tag{75}$$

To prove these lemmas we rewrite (49) and (50) as

$$\begin{aligned}
a &= x - cp + sq, && (76)\\
b &= y - sp - cq, && (77)\\
p &= -ca - sb + (cx + sy), && (78)\\
q &= sa - cb + (cy - sx). && (79)
\end{aligned}$$

We then assume that one of the points (a, b) or (p, q) is a sentinel and prove that the other satisfies (51) or (52), as appropriate.

Let us then continue with the proof of Lemma 10. If $(x, y)^t$ satisfies one of the conditions (68), (70) or (71) then Lemmas 18, 20 and 21 show that $d \in \mathcal{D}_\theta(S)$ and Lemmas 18, 24 and 25 show that $d \in \mathcal{D}_\theta(T)$. Otherwise the following conditions must hold:

$$\begin{aligned}
y &\leq s\lambda - 1. && (80)\\
-s(\lambda - 2\delta) - 1 < l = cy - sx &< s(\lambda - 2\delta) + 1.
\end{aligned}$$

We can then use Lemma 15 to get an integer $k \geq 2$ for which $(k\delta - \lambda, 0)^t \in S \cap T$ and such that

$$\phi = cy - sx - s(k\delta - \lambda) = l - s(k\delta - \lambda) \tag{81}$$

satisfies

$$|\phi| < 1. \tag{82}$$

Taking $a = -(k\delta - \lambda)$ and $b = 0$, we have $s = t = (a, b) \in S \cap T$, because $S = -S$ and $T = -T$. Moreover, the equations (78) and (79) lead to

$$\begin{aligned} p &= c(k\delta - \lambda) + cx + sy & (83)\\ q &= -s(k\delta - \lambda) + cy - sx = \phi & (84) \end{aligned}$$

and the items below prove that $r = (p, q)^t = d - H_\theta^{-1} s \in R$:

$$\begin{array}{lcll} p > -\lambda: & (83), (43) & \Rightarrow & p \geq c(k\delta - \lambda) = -c\lambda + ck\delta > \lambda. \\ p < \lambda: & (83) & \Rightarrow & sp = cs(k\delta - \lambda) + csx + s^2 y, \\ & (81) & \Rightarrow & sp = c(s(k\delta - \lambda) - cy + sx) + y = y - c\phi, \\ & (80) & \Rightarrow & sp \leq s\lambda - 1 - c\phi = -(1 + c\phi) + s\lambda, \\ & (82) & \Rightarrow & sp \leq -(1 - |\phi|) + s\lambda < s\lambda \Rightarrow p < \lambda. \\ |q| < 1: & (82), (84) & \Rightarrow & |q| = |\phi| < 1. \end{array}$$

Thus, we have shown that $(x, y)^t \in \mathcal{D}_\theta(S) \cap \mathcal{D}_\theta(T)$ and the proof of Lemma 10 is complete •

Proof of Lemma 11. If $d \in \mathcal{D}_\theta(-A)$ then either (I) $d = a + H_\theta r$ or (II) $d = r + H_\theta a$, with $r \in R$ and $a \in A$. In case (I) $d = -(-a + H_\theta(-r))$ and in case (II) $d = -(-r + H_\theta(-a))$, with $-r \in R$ and $-a \in -A$ in both cases. Therefore, $\mathcal{D}_\theta(-A) \subset -\mathcal{D}_\theta(A)$. Changing A by $-A$ we get $\mathcal{D}_\theta(A) = \mathcal{D}_\theta(- - A) \subset -\mathcal{D}_\theta(-A)$. This implies $-\mathcal{D}_\theta(A) \subset -\mathcal{D}_\theta(-A)$ and completes the proof •

Proof of Lemma 12. Let us define

$$c_h = \cos(\theta/2) \text{ and } s_h = \sin(\theta/2). \tag{85}$$

Notice that $1 + c = 2c_h^2$, $s = 2c_h s_h$ and $c_h > 0$, because, by hypothesis $-\pi/2 < \theta/2 < \pi/2$. As a consequence, by the definitions of Q_θ and $\tilde{Q}_\theta$ in (35) and (36),

$$\begin{aligned} Q_\theta &= \{(x, y) \in \mathcal{R}_\theta \text{ such that } c_h x + s_h y \geq 0 \text{ and } c_h y - s_h x \geq 0\}, & (86)\\ \tilde{Q}_\theta &= \{(x, y) \in \mathcal{R}_\theta \text{ such that } c_h x + s_h y \geq 0 \text{ and } c_h y - s_h x \leq 0\}. & (87) \end{aligned}$$

Taking K as the first quadrant of $I\!R^2$,

$$K = \{(x, y)^t \in I\!R^2 \text{ such that } x \geq 0 \text{ and } y \geq 0\},$$

and remembering that F, defined in (44), is the reflection on the x axis, we can rewrite (86) and (87) as

$$\begin{aligned} Q_\theta &= \{v \in \mathcal{R}_\theta \text{ such that } H_{-\theta/2} v \in K\}, & (88)\\ \tilde{Q}_\theta &= \{v \in \mathcal{R}_\theta \text{ such that } F H_{-\theta/2} v \in K\}. & (89) \end{aligned}$$

To complete this proof we assume that $\mathcal{D}_\theta(A) \supset Q_\theta$ and show that $\mathcal{D}_\theta(FA) \supset \tilde{Q}_\theta$. Take $d \in \tilde{Q}_\theta$. Since $d \in \mathcal{R}_\theta$, $d = u + H_\theta v$ for $u, v \in R$. Equation (89) shows that $FH_{-\theta/2} d \in K$. Therefore, $FH_{-\theta/2} u + FH_{\theta/2} v \in K$. This is equivalent to $FH_{-\theta/2} FFu + FH_{\theta/2} FFv \in K$.

Using the identity $FH_\alpha F = H_{-\alpha}$, we deduce that $H_{-\theta/2}(H_\theta Fu + Fv) \in K$. Thus, by (88), $H_\theta Fu + Fv \in Q_\theta$. By our assumption that $\mathcal{D}_\theta(A) \supset Q_\theta$ we have that either (I) $H_\theta Fu + Fv = a + H_\theta r$ or (II) $H_\theta Fu + Fv = r + H_\theta a$, with $r \in R$ and $a \in A$.

Notice that

$$d = u + H_\theta v = F(Fu + FH_\theta FFv) = F(Fu + H_{-\theta}Fv) = FH_{-\theta}(H_\theta Fu + Fv).$$

Therefore, in case (I)

$$d = FH_{-\theta}(a + H_\theta r) = FH_{-\theta}FFa + Fr = (Fr) + H_\theta(Fa)$$

and in case (II)

$$d = FH_{-\theta}(r + H_\theta a) = FH_{-\theta}FFr + Fa = (Fa) + H_\theta(Fr).$$

In both cases we see that $d \in \mathcal{D}_\theta(FA)$ and the lemma is proved •

Proof of Lemma 13. Given $d = u + H_{-\theta}v$ in $\mathcal{R}_{-\theta}$ we must show that $d \in \mathcal{D}_{-\theta}(FA)$. Notice that $Fd = Fu + FH_{-\theta}FFv = Fu + H_\theta Fv \in I_\theta$, because $FH_{-\theta}F = H_\theta$. Since we are assuming that $\mathcal{D}_\theta(A) = \mathcal{R}_\theta$, there are $r \in R$ and $a \in A$ such that either (I) $Fd = r + H_\theta\sigma$ or (II) $Fd = a + H_\theta r$. In case (I), multiplying by F we get

$$d = FFd = Fr + FH_\theta FF\sigma = (Fr) + H_{-\theta}(Fa) \in \mathcal{D}_{-\theta}(FA).$$

In case (II), multiplying by F we get

$$d = FFd = Fa + FH_\theta FFr = (Fa) + H_{-\theta}(Fr) \in \mathcal{D}_{-\theta}(FA).$$

Therefore, in both cases $d \in \mathcal{D}_{-\theta}(FA)$ and the proof of is complete •

Proof of Lemma 14. Given $d = u + H_{\theta+\pi}v$ with $u, v \in R$ we must show that $d \in \mathcal{D}_{\theta+\pi}(A)$. Notice that $d = u + H_\theta(-v) \in \mathcal{R}_\theta$, because $H_{\theta+\pi} = H_\pi H_\theta = -H_\theta$. Since, by hypothesis, $\mathcal{D}_\theta(A) = \mathcal{R}_\theta$, there are $r \in R$ and $a \in A$ such that either (I) $d = r + H_\theta a$ or (II) $d = a + H_\theta r$. In Case (I) we have $d = r + H_{\theta+\pi}(-a) \in \mathcal{D}_{\theta+\pi}(A)$ because $-a \in A$ since $-A = A$. In Case (II) $d = a + H_{\theta+\pi}(-r) \in \mathcal{D}_{\theta+\pi}(A)$ because $a \in A$ and $-r \in R$. Therefore, in both cases $d \in \mathcal{D}_{\theta+\pi}(A)$ and the proof of Lemma 14 is complete •

Proof of Lemma 15. In this proof we will use the identity

$$2\lambda = (n^\lambda + 2)\delta, \tag{90}$$

which can be derived by an analysis of (29) for $\lambda < 4$ and $\lambda \geq 4$. We have the following cases

$$l \leq -s(\lambda - 3\delta/2) \tag{91}$$
$$-s(\lambda - 3\delta/2) \leq l \leq 0. \tag{92}$$
$$l > 0 \tag{93}$$

which are analyzed as follows

Case 91: In this case we can take $k = 2$. In fact, $(2\delta - \lambda, 0)^t \in S \cap T$ and the hypothesis of this lemma implies $l - s(2\delta - \lambda) > -1$ and, since $\delta < 2$,

$$l \leq -s(\lambda - 3\delta/2) \Rightarrow l - s(2\delta - \lambda) \leq \delta/2 < 1.$$

and we have verified the condition $|l - s(k\delta - \lambda)| < 1$.

Case 92: We claim that the following k satisfies the conditions required by the present lemma:

$$k = \lceil \kappa \rceil \text{ where } \kappa = \frac{2s\lambda + 2l + s\delta}{2s\delta}. \tag{94}$$

By the definition of ceiling,

$$k = \kappa - \phi, \text{ with } 0 \leq \phi < 1.$$

Therefore, since $\delta < 2$ by (98) and $0 < s \leq 1$ by hypothesis,

$$|l - s(k\delta - \lambda)| = |l - s((\kappa - \phi)\delta - \lambda)| = |s\phi - \frac{1}{2}|\delta < \frac{1}{2} \times 2 = 1. \tag{95}$$

The definition of k and κ, the condition (92) and equation (29) lead to

$$\kappa \leq \frac{2\lambda + \delta}{2\delta} = \frac{(n^\lambda + 2)\delta + \delta}{2\delta} = \frac{n^\lambda}{2} + 1 \leq n^\lambda. \tag{96}$$

$$\kappa \geq \frac{2s\lambda + s\delta - 2s(\lambda - 3\delta/2)}{2s\delta} = 2. \tag{97}$$

The last two equations show that $(k\delta - \lambda, 0)^t \in S \cap T$, because $2 \leq k = \lfloor \kappa \rfloor \leq n^\lambda$. This, together with (95) shows that the k given by (94) is valid.

Case 92: From the previous cases, there exists $\tilde{k}$ such that $|-l - (\tilde{k}\delta - \lambda)| < 1$ and $2 \leq \tilde{k} \leq n^\lambda$. Take $k = n^\lambda + 2 - \tilde{k}$. It is clear that $2 \leq k \leq n^\lambda$. Thus, using (29), we get

$$\begin{aligned}|l - (k\delta - \lambda)| &= |l - ((n^\lambda + 2 - \tilde{k})\delta - \lambda)| = |-(-l - (\tilde{k}\delta - \lambda)) - ((n^\lambda + 2)\delta - 2\lambda)| \\ &= |-(-l - (\tilde{k}\delta - \lambda))| = |-l - (\tilde{k}\delta - \lambda)| < 1.\end{aligned}$$

We have analyzed all possibilities and the proof is complete •

Now, let us prove lemmas 16 — 24. Along these proofs we will use the bound

$$\delta < 2, \tag{98}$$

$$\delta \leq \lambda/2 \tag{99}$$

which can be deduced considering the cases $\lambda < 4$ and $\lambda \geq 4$ and (25) and (26). These lemmas assume $0 < c, s < 1$ and we will use the following bounds on $(x, y)^t \in Q_\theta$:

$$cy - sx \leq y, \tag{100}$$

$$cy - sx \geq -y \tag{101}$$

$$sy \geq (1 - c)x, \tag{102}$$

$$s(cy - sx) \geq (c - 1)(cx + sy), \tag{103}$$

$$(1 - c)(cy - sx) \leq s(cx + sy), \tag{104}$$

$$(1 - c)(cx + sy) \leq sy. \tag{105}$$

These bounds are consequence of the definition of Q_θ in (35) and the identities:

$$
\begin{aligned}
(100) &\quad : \quad cy - sx = y - \frac{s}{1+c}((1+c)x + sy),\\
(101) &\quad : \quad cy - sx = -y + ((1+c)y - sx),\\
(102) &\quad : \quad sy = (1-c)x + \frac{s}{1+c}((1+c)y - sx)\\
(103) &\quad : \quad s(cy - sx) = -(1-c)(cx+sy) + \frac{s}{1+c}((1+c)y - sx),\\
(104) &\quad : \quad (1-c)(cy - sx) = s(cx+sy) - \frac{s}{1+c}((1+c)x + sy),\\
(105) &\quad : \quad (1-c)(cx+sy) = sy - \frac{cs}{1+c}((1+c)y - sx).
\end{aligned}
$$

Proof of Lemma 16. Given $d \in Q_\theta$ satisfying (66), if we take $(a,b)^t = (\lambda, 1)^t \in S \cap T$, then p and q given by (78) and (79) satisfy

$$p = -c\lambda - s + (cx + sy), \tag{106}$$
$$q = s\lambda - c + (cy - sx). \tag{107}$$

The items below prove that $(p,q)^t \in R$, showing that $d \in \mathcal{D}_\theta(S) \cap \mathcal{D}_\theta(T)$.

$$
\begin{array}{lll}
p > -\lambda: \ (106),(104) & \Rightarrow & sp = -cs\lambda - s^2 + s(cx+sy) \geq -cs\lambda - s^2 + (1-c)(cy - sx)\\
\qquad\qquad (66) & \Rightarrow & sp > -cs\lambda - s^2 + (1-c)(1+c-s\lambda) = -s\lambda \Rightarrow p > -\lambda.\\
p < \lambda: \quad (106),(41) & \Rightarrow & p < -c\lambda - s + ((1+c)\lambda + s) = \lambda.\\
q > -1: \ (107),(103) & \Rightarrow & sq = s(s\lambda - c) + s(cy - sx)\\
 & \Rightarrow & sq \geq s(s\lambda - c) - (1-c)(cx+sy)\\
\qquad\qquad (41) & \Rightarrow & sq > s(s\lambda - c) - (1-c)((1+c)\lambda + s) = -s \Rightarrow q > -1.\\
q < 1: \quad (107),(66) & \Rightarrow & q < (s\lambda - c) + (1 + c - s\lambda) = 1.
\end{array}
$$

Proof of Lemma 17. Consider $(x,y)^t \in Q_\theta$. If x and y satisfy (66) then Lemma 16 shows that $(x,y)^t \in \mathcal{D}_\theta(S) \cap \mathcal{D}_\theta(T)$. Otherwise, we have that

$$cy - sx \geq 1 + c - s\lambda. \tag{108}$$

Taking $(p,q)^t = (\lambda,1)^t \in S \cap T$ and a,b as in (76) and (77) we get

$$a = x - c\lambda + s, \tag{109}$$
$$b = y - s\lambda - c. \tag{110}$$

The items below prove that $(a,b)^t \in R$, showing that $(x,y)^t \in \mathcal{D}_\theta(S) \cap \mathcal{D}_\theta(T)$.

$$
\begin{array}{lll}
a > -\lambda: \quad (109) & \Rightarrow & sa = sx - cs\lambda + s^2 = cy - (cy - sx) - cs\lambda + s^2\\
\qquad\qquad (100) & \Rightarrow & sa \geq (c-1)y - cs\lambda + s^2\\
\qquad\qquad (40) & \Rightarrow & sa > (c-1)(1 + c + s\lambda) - cs\lambda + s^2 = -s\lambda \Rightarrow a > -\lambda.\\
a < \lambda: \quad (109) & \Rightarrow & sa = sx - cs\lambda + s^2 = cy + (sx - cy) - cs\lambda + s^2\\
\qquad\qquad (108) & \Rightarrow & sa \leq cy - 1 - c + s\lambda - cs\lambda + s^2\\
\qquad\qquad (40) & \Rightarrow & sa < c(1 + s\lambda + c) - 1 - c + s\lambda - cs\lambda + s^2 = s\lambda \Rightarrow a < \lambda.\\
b > -1: \ (110),(67) & \Rightarrow & b > -1.\\
b < 1: \quad (110),(40) & \Rightarrow & b < 1.
\end{array}
$$

Proof of Lemma 18. Consider $(x,y)^t \in Q_\theta$. If x and y satisfy either (66) or (67) then Lemmas 16 and 17 show that $(x,y)^t \in \mathcal{D}_\theta(S) \cap \mathcal{D}_\theta(T)$. Otherwise, we must have

$$\begin{aligned} cy - sx &\geq 1 + c - s\lambda. && (111) \\ y &\leq s\lambda + c - 1. && (112) \end{aligned}$$

Taking $(p,q)^t = (\lambda, 0)^t \in S \cap T$ and a and b as in (76) and (77) we get

$$\begin{aligned} a &= x - c\lambda && (113) \\ b &= y - s\lambda. && (114) \end{aligned}$$

The items below prove that $(a,b)^t \in R$, showing that $(x,y)^t \in \mathcal{D}_\theta(S) \cap \mathcal{D}_\theta(T)$.

$$\begin{array}{lcll} a > -\lambda : & (113) & \Rightarrow & sa = sx - cs\lambda \geq cy - (cy - sx) - cs\lambda. \\ & (100),(112) & \Rightarrow & sa \geq (c-1)y - cs\lambda > (c-1)(s\lambda - 1) - cs\lambda \\ & & \Rightarrow & sa \geq -s\lambda + 1 - c > -s\lambda \Rightarrow a > -\lambda. \\ a < \lambda : & (113) & \Rightarrow & sa = sx - cs\lambda = cy + (sx - cy) - cs\lambda \\ & (111) & \Rightarrow & sa \leq cy - 1 - c + s\lambda - cs\lambda \\ & (112) & \Rightarrow & sa \leq c(c + s\lambda - 1) - 1 - c + s\lambda - cs\lambda = s\lambda - s^2 - 2c \\ & & \Rightarrow & a < \lambda. \\ b > -1 : & (114),(68) & \Rightarrow & b > -1. \\ b < 1 : & (114),(112) & \Rightarrow & b \leq c - 1 < 1. \end{array}$$

Proof of Lemma 19. Consider $(x,y)^t \in Q_\theta$. If $s\delta \leq c$ then the hypothesis (69) implies

$$y > s(\lambda - \delta) + c - 1 \geq s\lambda - 1$$

and in this case Lemma 18 shows that $(x,y)^t \in \mathcal{D}_\theta(S)$. Therefore, using the hypothesis that $c > 0$, we assume from now on that

$$s\delta > c > 0. \qquad (115)$$

If x and y satisfy either (66) or (68) then Lemmas 16 and 18 show that $(x,y)^t \in \mathcal{D}_\theta(S)$. Otherwise we have

$$\begin{aligned} cy - sx &\geq 1 + c - s\lambda. && (116) \\ y &\leq s\lambda - 1. && (117) \end{aligned}$$

Taking $v = (p,q)^t = (\lambda - \delta, 1)^t \in S$ and a and b as in (76) and (77) we get

$$\begin{aligned} a &= x - c(\lambda - \delta) + s && (118) \\ b &= y - s(\lambda - \delta) - c. && (119) \end{aligned}$$

The items below prove that $(a,b)^t \in R$, showing that $(x,y)^t \in \mathcal{D}_\theta(S)$.

$$\begin{array}{lccl}
a > -\lambda: & (118) & \Rightarrow & sa = sx - cs(\lambda-\delta) + s^2 \\
& & \Rightarrow & sa = cy - (cy - sx) - cs(\lambda-\delta) + s^2 \\
& (100),(117) & \Rightarrow & sa \geq (c-1)(s\lambda - 1) - cs(\lambda-\delta) + s^2 \\
& (115) & \Rightarrow & sa \geq -s\lambda + 1 - c + s^2 + cs\delta \\
& & \Rightarrow & sa \geq -s\lambda + 1 - c + s^2 + c^2 \\
& & \Rightarrow & sa \geq -s\lambda + 2 - c \Rightarrow a > -\lambda. \\
a < \lambda: & (118) & \Rightarrow & sa = sx - cs(\lambda-\delta) + s^2 \\
& & \Rightarrow & sa = cy - (cy - sx) - cs(\lambda-\delta) + s^2 \\
& (116),(117) & \Rightarrow & sa \leq c(s\lambda - 1) - 1 - c + s\lambda - cs(\lambda-\delta) + s^2 \\
& (98),(115) & \Leftrightarrow & sa \leq s\lambda - (1 + 2c - cs\delta - s^2) \\
& (115) & \Rightarrow & sa < s\lambda - c(c + 2 - 2s) < s\lambda \Rightarrow a < \lambda. \\
b > -1: & (119),(69) & \Rightarrow & b > -1. \\
b < 1: & (119),(117),(98) & \Rightarrow & b \leq -1 - c + \delta s < 2s - 1 - c \leq 1 \Rightarrow b < 1.
\end{array}$$

Proof of Lemma 20. Consider $(x,y)^t \in Q_\theta$. If x and y satisfy (66) or (68) then Lemmas 16 and 18 show that $(x,y)^t \in \mathcal{D}_\theta(S)$. Otherwise we have

$$cy - sx \geq 1 + c - s\lambda, \tag{120}$$

$$y \leq s\lambda - 1. \tag{121}$$

Taking $u = (a,b)^t = (\lambda - \delta, 1)^t \in S$ and p and q as in (78) and (79) we get

$$p = -c(\lambda-\delta) - s + (cx + sy) \tag{122}$$

$$q = s(\lambda-\delta) - c + (cy - sx). \tag{123}$$

and the items below prove that $(p,q)^t \in R$, showing that $(x,y)^t \in \mathcal{D}_\theta(S)$.

$$\begin{array}{lccl}
p > -\lambda: & (122) & \Rightarrow & (1-c)p = -(1-c)(c(\lambda-\delta) + s) + (1-c)(cx + sy) \\
& (103) & \Rightarrow & (1-c)p \geq -(1-c)(c(\lambda-\delta) + s) - s(cy - sx) \\
& (70) & \Rightarrow & (1-c)p \geq -(1-c)(c(\lambda-\delta) + s) + s(s(\lambda - 2\delta) + 1) \\
& & \Rightarrow & (1-c)p \geq -(1-c)\left(c(\lambda-\delta) - (1+c)(\lambda - 2\delta)\right) + cs \\
& (99) & \Rightarrow & p > -(1+c)\delta + (\lambda - \delta) \geq -(1+c)\lambda/2 + \lambda/2 \geq -c\lambda/2 > -\lambda. \\
p < \lambda: & (122) & \Rightarrow & (1-c)p = -(1-c)c(\lambda-\delta) - (1-c)s + (1-c)(cx + sy) \\
& (105) & \Rightarrow & (1-c)p \leq -(1-c)c(\lambda-\delta) - (1-c)s + sy \\
& (121) & \Rightarrow & (1-c)p \leq -(1-c)c(\lambda-\delta) - (1-c)s + s(s\lambda - 1) \\
& & \Rightarrow & (1-c)p \leq (1-c)\lambda + c(1-c)\delta - (2-c)s \\
& & \Rightarrow & (1-c)p < (1-c)\lambda + 2c(1-c) - (2-c)s \\
& & \Rightarrow & (1-c)p < (1-c)\lambda - \frac{1-c}{s}((2-c)(1+c) - 2cs) \\
& & \Rightarrow & (1-c)p < (1-c)\lambda - \frac{1-c}{s}(2(1-cs) + c(1-c)) \leq (1-c)\lambda \\
& & \Rightarrow & p < \lambda. \\
q > -1: & (123),(120) & \Rightarrow & q \geq s(\lambda-\delta) - c + 1 + c - s\lambda \\
& (98) & \Rightarrow & q \geq 1 - s\delta > 1 - 2s > -1 \Rightarrow q > -1. \\
q < 1: & (123),(70) & \Rightarrow & q \leq s(\lambda-\delta) - c - s(\lambda - 2\delta) - 1 \\
& (98) & \Rightarrow & q \leq \delta s - 1 - c < 2s - 1 \leq 1 \Rightarrow q < 1.
\end{array}$$

Proof of Lemma 21. Consider $(x,y)^t \in Q_\theta$. If $s\delta \leq 2-c$ then (100) and the hypothesis (68) imply

$$y \geq cy - sx > s(\lambda - 2\delta) + 1 = s(\lambda-\delta) + 1 - \delta s \geq s(\lambda-\delta) + c - 1$$

and the present lemma follows from lemma 19. Therefore, we may assume that

$$s\delta \geq 2 - c. \tag{124}$$

If x and y satisfy (69) then lemma 19 shows that $d \in \mathcal{D}_\theta(S)$. Otherwise we have

$$y \quad \leq \quad s(\lambda-\delta) + c - 1. \tag{125}$$

Taking $u = (a,b)^t = -(\lambda-\delta, 1)^t \in S$ and p and q as in (78) and (79) we get

$$p \quad = \quad c(\lambda-\delta) + s + (cx+sy) \tag{126}$$
$$q \quad = \quad -s(\lambda-\delta) + c + (cy - sx). \tag{127}$$

The items below prove that $(p,q)^t \in R$, showing that $(x,y)^t \in \mathcal{D}_\theta(S)$.

$$\begin{array}{lcll}
p > -\lambda: & (126),(43) & \Rightarrow & p \geq 0 > -\lambda. \\
p < \lambda: & (126) & \Rightarrow & sp = cs(\lambda-\delta) + s^2 - c(cy-sx) + y \\
 & (71) & \Rightarrow & sp \leq s^2 + cs\delta - c + y \\
 & (125) & \Rightarrow & sp \leq s\lambda - (1-c)s\delta - c + c - 1 + s^2 \\
 & (124) & \Rightarrow & sp \leq s\lambda - (1-c)s\delta - c^2 \Rightarrow p < \lambda. \\
q > -1: & (127),(71),(98) & \Rightarrow & q \geq 1 - \delta s + c > 1 - 2s + c \geq -1 \Rightarrow q > -1. \\
q < 1: & (127),(100) & \Rightarrow & q \leq c - s(\lambda-\delta) + y \\
 & (125) & \Rightarrow & q \leq 2c - 1 < 1.
\end{array}$$

Proof of Lemma 22. Consider $(x,y)^t \in Q_\theta$. If x and y satisfy (68) then Lemma 18 shows that $(x,y)^t \in \mathcal{D}_\theta(T)$. Otherwise we have

$$y \quad \leq \quad s\lambda - 1. \tag{128}$$

Taking $u = (a,b)^t = -(\lambda-\delta, -1)^t \in T$ and p and q as in (78) and (79) we get

$$p \quad = \quad c(\lambda-\delta) - s + (cx+sy) \tag{129}$$
$$q \quad = \quad -s(\lambda-\delta) - c + (cy - sx). \tag{130}$$

The items below prove that $(p,q)^t \in R$, showing that $(x,y)^t \in \mathcal{D}_\theta(T)$.

$$\begin{array}{lcll}
p > -\lambda: & (129),(43) & \Rightarrow & p > -s > -1 > -\lambda. \\
p < \lambda: & (129) & \Rightarrow & sp = cs(\lambda-\delta) - s^2 + c(sx-cy) + y \\
 & (72) & \Rightarrow & sp \leq cs(\lambda-\delta) - s^2 - cs(\lambda-2\delta) - c^2 + c + y \\
 & (128) & \Rightarrow & sp \leq (cs\delta - 1) + c + s\lambda - 1 = s\lambda - (1-c) - (1-2cs) \Rightarrow p < \lambda. \\
q > -1: & (130),(72) & \Rightarrow & q > -1. \\
q < 1: & (130),(100),(128) & \Rightarrow & q \leq y - s(\lambda-\delta) - c < s(\lambda-1) - s(\lambda-\delta) - c < s - c < 1.
\end{array}$$

Proof of Lemma 23. Consider $(x,y)^t \in Q_\theta$. If d satisfies either (66), (68) or (72) then Lemmas 16, 18 and 22 show that $d \in \mathcal{D}_\theta(T)$. Otherwise d satisfies

$$\begin{aligned} cy - sx &\geq 1 + c - s\lambda, && (131)\\ y &\leq s\lambda - 1. && (132)\\ cy - sx &\leq s(\lambda-\delta) + c - 1. && (133) \end{aligned}$$

Taking $v = (p,q)^t = (\lambda, -1)^t \in T$ and a and b as in (76) and (77) we get

$$\begin{aligned} a &= x - c\lambda - s && (134)\\ b &= y - s\lambda + c. && (135) \end{aligned}$$

The items below prove that $(a,b)^t \in R$, showing that $(x,y)^t \in \mathcal{D}_\theta(T)$.

$$\begin{array}{lcll} a > -\lambda: & (134) & \Rightarrow & sa = cy - (cy - sx) - s(c\lambda + s) \\ & (133) & \Rightarrow & sa \geq cy + 1 - c - s(\lambda-\delta) - cs\lambda - s^2 \\ & (73) & \Rightarrow & sa \geq c(s(\lambda-\delta) - c + 1) + c^2 - c - s(\lambda-\delta) - cs\lambda \\ & & \Leftrightarrow & sa \geq -s\lambda + (1-c)s\delta \Rightarrow a > -\lambda. \\ a < \lambda: & (134) & \Rightarrow & sa = cy - (cy - sx) - s(c\lambda + s) \\ & (132) & \Rightarrow & sa \leq c(s\lambda - 1) - (cy - sx) - s(c\lambda + s) \\ & (131) & \Rightarrow & sa \leq -c - s^2 - (1 + c - s\lambda) \\ & & \Leftrightarrow & sa \leq s\lambda - (1 + 2c + s^2) \Rightarrow a < \lambda. \\ b > -1: & (135), (73) & \Rightarrow & b \geq (s(\lambda-\delta) + 1 - c) - s\lambda + c \\ & (98) & \Rightarrow & b \geq 1 - \delta s > 1 - 2s \geq -1 \Rightarrow b > -1. \\ b < 1: & (135), (132) & \Rightarrow & b \leq c - 1 < 1. \end{array}$$

Proof of Lemma 24. Consider $(x,y)^t \in Q_\theta$. If $s\delta \leq 1 + c/2$ then the hypothesis (74) implies $cy - sx < -s\lambda + 2s\delta - 1 \leq 1 + c - s\lambda$ and the present lemma follows from Lemma 16. Thus we can assume that

$$s\delta > 1 + c/2. \qquad (136)$$

If x and y satisfy (72) or (73) then lemmas 22 and 23 show that $(x,y)^t \in \mathcal{D}_\theta(T)$. Otherwise we have

$$\begin{aligned} cy - sx &\leq s(\lambda-\delta) + c - 1. && (137)\\ y &< s(\lambda-\delta) + 1 - c. && (138) \end{aligned}$$

Taking $v = (p,q)^t = (\lambda - \delta, -1)^t \in T$ and a b as in (76) and (77) we get

$$\begin{aligned} a &= x - c(\lambda-\delta) - s, && (139)\\ b &= y - s(\lambda-\delta) + c. && (140) \end{aligned}$$

The items below prove that $(a,b)^t \in R$, showing that $(x,y)^t \in \mathcal{D}_\theta(T)$.

$$
\begin{array}{llcl}
a > -\lambda: & (139) & \Rightarrow & sa = sx - s(c(\lambda-\delta)+s) \\
 & & \Leftrightarrow & sa = cy - (cy - sx) - s(c(\lambda-\delta)+s) \\
 & (100) & \Rightarrow & sa \geq (c-1)(cy-sx) - s(c(\lambda-\delta)+s) \\
 & (137) & \Rightarrow & sa \geq -(1-c)(s(\lambda-\delta)+c-1) - s(c(\lambda-\delta)+s) \\
 & & \Rightarrow & sa \geq -s\lambda + s\delta + (1-c)^2 - s^2 = -s\lambda + s\delta + 2c^2 - 2c \\
 & (136) & \Rightarrow & sa > -s\lambda + 1 - 2c + c^2 + c^2 + c/2 \geq -s\lambda + (1-c)^2 \\
 & & \Rightarrow & a > -\lambda. \\
a < \lambda: & (139) & \Rightarrow & (1-c)a = (1-c)x - (1-c)(c(\lambda-\delta)+s) \\
 & (102),(137) & \Rightarrow & (1-c)a \leq s(s(\lambda-\delta)+1-c) - (1-c)(c(\lambda-\delta)+s) \\
 & & \Rightarrow & (1-c)a \leq (1-c)(\lambda-\delta) \Rightarrow a < \lambda. \\
b > -1: & (140),(101) & \Rightarrow & b \geq -(cy-sx) - s(\lambda-\delta) + c \\
 & (74) & \Rightarrow & b \geq s(\lambda-2\delta) + 1 - s(\lambda-\delta) + c \\
 & (98) & \Rightarrow & b \geq 1 + c - \delta s > 1 + c - 2s \geq -1 \Rightarrow b > -1. \\
b < 1: & (140),(138) & \Rightarrow & b < 1.
\end{array}
$$

Proof of Lemma 25. Consider $(x,y)^t \in Q_\theta$. If $s\delta < 2-c$ then the hypothesis (75) implies that

$$cy - sx \geq s(\lambda-2\delta)+1 = s(\lambda-\delta)+1-s\delta > s(\lambda-\delta)+c-1$$

and this lemma follows from lemma 16. Therefore, we can assume that

$$s\delta \geq 2-c. \tag{141}$$

If x and y satisfy (72) or (73) then Lemmas 22 and 23 show that $(x,y)^t \in \mathcal{D}_\theta(T)$. Otherwise we have

$$
\begin{aligned}
cy - sx &\leq s(\lambda-\delta)+c-1, &(142)\\
y &< s(\lambda-\delta)+1-c. &(143)
\end{aligned}
$$

Taking $v = (p,q)^t = (\lambda-\delta,-1)^t \in T$ and a and b as in (76) and (77) we get

$$
\begin{aligned}
a &= x - c(\lambda-\delta) - s &(144)\\
b &= y - s(\lambda-\delta) + c &(145)
\end{aligned}
$$

and the items below prove that $(a,b)^t \in R$, showing that $(x,y)^t \in \mathcal{D}_\theta(T)$.

$$
\begin{array}{llll}
a > -\lambda: & (144) & \Rightarrow & sa = sx - s(c(\lambda-\delta)+s) \\
 & & \Leftrightarrow & sa = cy - (cy - sx) - s(c(\lambda-\delta)+s) \\
 & (100) & \Rightarrow & sa \geq (c-1)(cy-sx) - s(c(\lambda-\delta)+s) \\
 & (142) & \Rightarrow & sa \geq (c-1)(s(\lambda-\delta)+c-1) - s(c(\lambda-\delta)+s) \\
 & & \Rightarrow & sa \geq -s\lambda + s\delta + (1-c)^2 - s^2 = -s\lambda + s\delta + 2c^2 - 2c \\
 & (141) & \Rightarrow & sa \geq -s\lambda + 2 - 3c + 2c^2 \\
 & & \Rightarrow & sa \geq -s\lambda + 2(1-c)^2 + c > -s\lambda \Rightarrow a > -\lambda. \\
a < \lambda: & (144) & \Rightarrow & (1-c)a = (1-c)x - (1-c)(c(\lambda-\delta)+s) \\
 & (102),(142) & \Rightarrow & (1-c)a \leq s(s(\lambda-\delta)+1-c) - (1-c)(c(\lambda-\delta)+s) \\
 & & \Rightarrow & (1-c)a \leq (1-c)(\lambda-\delta) \Rightarrow a < \lambda. \\
b > -1: & (145),(100) & \Rightarrow & b \geq cy - sx - s(\lambda-\delta) + c \\
 & (75) & \Rightarrow & b \geq 1 + c - s\delta \\
 & (98) & \Rightarrow & b > 1 + c - 2s \geq -1 \Rightarrow b > -1. \\
b < 1: & (144),(143) & \Rightarrow & b < 1.
\end{array}
$$

References

[1] C. Amaral, J. Bernardo and J. Jorge, Marker making using automatic placement of irregular shapes for the garment industry, *Computers and Graphics* 14, pp. 41–46, 1990.

[2] M. Arenales and R. Morabito, An and/or-graph approach to the solution of two-dimensional non-guillotine cutting problems, *European Journal of Operational Research* 84, pp. 599–617, 1995.

[3] J. E. Beasley, An exact two-dimensional non-guillotine cutting tree search procedure, *Operations Research* 33, pp. 49-64, 1995.

[4] J. E. Beasley, A population heuristic for constrained two-dimensional non-guillotine cutting, *European Journal of Operational Research*, to appear.

[5] J. A. Bennell, K. A. Dowsland and W. B. Dowsland, The irregular cutting-stock problem - a new procedure for deriving the non-fit polygon, *Computers & Operations Research* 28, pp. 271-287, 2001.

[6] E. G. Birgin and J. M. Martínez, Large-scale active-set box-constrained optimization method with spectral projected gradients, *Computational Optimization and Applications* 23, pp. 101–125, 2002.

[7] E. G. Birgin, J. M. Martínez and M. Raydan, Nonmonotone spectral projected gradient methods on convex sets, *SIAM Journal on Optimization* 10, pp. 1196–1211, 2000.

[8] E. G. Birgin, J. M. Martínez and M. Raydan, Algorithm 813 SPG: Software for convex-constrained optimization, *ACM Transactions on Mathematical Software* 27, pp. 340–349, 2001.

[9] E. G. Birgin, J. M. Martínez and D. P. Ronconi, Optimizing the Packing of Cylinders into a Rectangular Container: A Nonlinear Approach, *European Journal of Operational Research*, to appear.

[10] E. Bischoff and W. B. Dowsland, An Application of the Micro to Product Design and Distribution, *Journal of the Operational Research Society* 33, pp. 271–280, 1982.

[11] E. Bischoff and M. Ratcliff, Loading multiple pallets, *Journal of the Operational Research Society* 46, pp. 1322–1336, 1995.

[12] C. S. Chen, S. M. Lee and Q. S. Shen, An analytical model for the container loading problem, *European Journal of Operational Research* 80, pp. 68-76, 1995.

[13] N. Christofides and E. Hadjiconstantinou, An exact algorithm for orthogonal 2-D cutting problems using guillotine cuts, *European Journal of Operational Research* 83, pp. 21–38, 1995.

[14] H. Dyckhoff, A typology of cutting and packing problems, *European Journal of Operational Research* 44, pp. 145–159, 1990.

[15] K. A. Dowsland, An exact algorithm for the pallet loading problem, *European Journal of Operational Research* 84, pp. 78–84, 1987.

[16] K. A. Dowsland, W. B. Dowsland and J. A. Bennell, Jostling for position - Local improvement for irregular cutting patterns. *Journal of the Operational Research Society* 49, pp. 647–658, 1998.

[17] K. A. Dowsland, S. Vaid and W. B. Dowsland, An algorithm for polygon placement using a bottom-left strategy, *European Journal of Operational Research* 141, pp. 371–381, 2002.

[18] P. Erdös and R. L. Graham, On packing squares with equal squares, *Journal of Combinatorial Theory A* 19, 119–123, 1975.

[19] E. Friedman, Packing unit squares into squares, *The electronic Journal of Combinatorics* 7, DS#7, 2000.

[20] E. Hadjiconstantinou and N. Christofides, An exact algorithm for general, orthogonal two-dimensional knapsack problems, *European Journal of Operational Research* 83, pp. 39–56, 1995.

[21] T. Hodgson, A combined approach to the pallet loading problem, *IIE Transactions* 14, pp. 176–182, 1982.

[22] H. Lamousin and W. N. Waggenspack Jr., Nesting of two-dimensional irregular parts using a shape reasoning heuristic, *Computer-Aided Design* 29, pp. 221–238, 1997.

[23] Z. Li and V. Milenkovic, Compaction and separation algorithms for non convex polygons and their application, *European Journal of Operational Research* 84, pp. 539–561, 1995.

[24] L. Lins, S. Lins and R. Morabito, An L-approach for packing (l,w)- rectangles into rectangular and L-shaped pieces, *Journal of the Operational Research Society*, to appear.

[25] J. H. Mahoney, Intermodal Freight Transportation, Eno Foundation for Transportation, Inc. Westport, Connecticut, 1985.

[26] J. M. Martínez and L. Martínez, Packing optimization for automated generation of complex system's initial configurations for molecular dynamics and docking. *Journal of Computational Chemistry* 24, pp. 819–825, 2003.

[27] R. Morabito and M. Arenales, An and/or-graph approach to the container loading problem, *International Transactions in Operational Research* 1, pp. 59–73, 1994.

[28] R. Morabito and S. Morales, A simple and effective recursive procedure for the manufacturer's pallet loading problem, *Journal of the Operational Research Society* 49, pp. 819–828, 1998.

[29] R. Morabito, S. Morales and J. A. Widmer, Loading optimization of palletized products on trucks, *Transportation Research* Part E 36, pp. 285–296, 2000.

[30] J. Nelissen, How to use the structural constraints to compute an upper bound for the pallet loading problem, *European Journal of Operational Research* 84, pp. 662–680, 1995.

[31] G. L. Nemhauser and L. A. Wosley, *Integer and Combinatorial Optimization*, Wiley, 1988.

[32] A. Tarnowski, J. Terno and G. Scheithauer, A polynomial-time algorithm for the guillotine pallet loading problem, *INFOR* 32, pp. 275–287, 1994.

[33] R. D. Tsai, E. M. Malstrom and W. Kuo, Three dimensional palletization of mixed box sizes, *IIE Transactions* 25, pp. 64–75, 1993.

[34] A. C. G. Viana and M. Arenales, O Problema de Corte de Placas Defeituosas, *Pesquisa Operacional*, to appear.